Devi Geetha Nair

Calorimetric Power Loss Measurement of a Small Power Converter

School of Electrical Engineering

Thesis submitted for examination for the degree of Master of Science in Technology.

Espoo 18.05.2012

Thesis supervisor:

Prof. Antero Arkkio

Thesis advisor:

DSc. (Tech.) Paavo Rasilo

Aalto University
School of Electrical
Engineering

AALTO UNIVERSITY
SCHOOL OF ELECTRICAL ENGINEERING

ABSTRACT OF THE
MASTER'S THESIS

Author: Devi Geetha Nair

Title: Calorimetric Power Loss Measurement of a Small Power Converter

Date: 18.05.2012 Language: English Number of pages:9+47

Department of Electrical Engineering

Professorship: Electromechanics Code: S-17

Supervisor: Prof. Antero Arkkio

Advisor: DSc. (Tech.) Paavo Rasilo

Miniaturisation – is the key word in technology today and the general trend in all industries is to seek for smaller and compact electrical and magnetic components. With the increase in energy density, the loss density does too, and so does the need to achieve greater measurement accuracy of device losses. Calorimeters are the way to accomplish this effectively, as proven by the prevailing calorimetric watt-meters for electrical systems.

The undertaking of this thesis work was to build a simple yet accurate calorimetric system to measure power losses in highly efficient power converters and similar small devices belonging to a power class of <1kW. An improved closed, water cooled calorimeter with flow control and input water temperature control has been implemented, as an alternative to the accepted, yet complicated double jacketed calorimeter. The balance tests with the calorimeter yielded the calibration curve, which was followed by the actual test with a 0.75 kW frequency converter. From the power losses measured by the calorimeter, the tested device was confirmed to have a high efficiency of 97%.

The calorimeter that was built is characterised by low flow rates and can measure loss powers in range of 25W-520W with an accuracy better than 1.5% for power losses <50W.

Keywords: Low Power Loss, Accurate Loss Measurement, Calorimeter, Small Power Converters.

Acknowledgments

The journey to the completion of this thesis work has been eventful and marked with contributions from a lot of people. Firstly, I would like to thank Prof. Antero Arkkio for entrusting me with this work and seeing me through till its completion. For sharing their valuable experience and knowledge, which enabled this work to take off and land safely, my supervisors Paavo Rasilo and Deepak Singh have my gratitude. I am ever grateful to Ari Haavisto for his helpfulness, support and suggestions in building the calorimeter and implementing its systems and Sami for making this work take shape and become a reality by building the calorimeter box. I appreciate my colleagues and friends in the Group of Electromechanics for creating a congenial work environment, which was crucial for this thesis to meet its successful completion.

My friends in India and Finland and from elsewhere on the globe, I thank you all for your constant encouragement and love. Lastly but most importantly I have my parents to thank, for making all of this possible for their daughter.

Otaniemi, 18.05.2013

Devi Geetha Nair.

Contents

List of Figures

List of Tables

Symbols and abbreviations

Symbols

ΔP_{in}	Absolute error in input power
ΔP_{loss}	Absolute error in power loss
ΔP_{out}	Absolute error in output power
ΔT	Temperature difference
η	Efficiency
κ	Thermal conductivity of copper
λ	Thermal conductivity of walls
ρ	Resistivity
ρ	Density
τ	Thermal time-constant
A	Area of cross-section
A_{cu}	Area of cross-section of copper conductor
A_{wall}	Surface area of the wall
C	Heat capacity rate
c_p	Specific heat capacity
C_{th}	Thermal capacity
d_{wall}	Wall thickness
f_{crit}	Critical frequency
f_{sw}	Switching frequency
I	Current
l	Length of the conductor
m	Mass of the quantity
N_{cu}	Number of copper conductors
p	Power density in copper conductor
P_{a}	Power transferred from air
P_{cond}	Conduction loss
P_{cu}	Power loss through copper connections
P_{fix}	Fixed power loss
P_{in}	Input power
P_{loss}	Total power loss of device
P_{out}	Output power
P_{stray}	Stray power loss
P_{sw}	Switching power loss
P_{wall}	Heat leakage losses
$P_{\text{water}}, P_{\text{w}}$	Power absorbed by water
Q	Heat energy
$\dot{Q}$	Rate of heat transfer
R	Resistance
R_{cu}	Copper thermal resistance
R_{th}	Thermal resistance

$R_{\mathrm{th,eq}}$	Equivalent thermal resistance
$R_{\mathrm{th,fc}}$	Thermal resistance of floor and ceiling
$R_{\mathrm{th,wall1}}$	Thermal resistance of wall 1
$R_{\mathrm{th,wall2}}$	Thermal resistance of wall 2
T_{Acold}	Cold air temperature exiting the heat exchanger
T_{amb}	Ambient temperature
T_{ch}	Temperature inside calorimeter chamber
T_{in}	Calorimetric chamber temperature
T_{out}	Outside ambient temperature
T_{Wcold}	Cold water temperature entering the heat exchanger
T_{Whot}	Hot water temperature entering the heat exchanger
$u_{\mathrm{P_{loss}}}$	Uncertainty in power loss measurement
V	Volume
$\dot{V}$	Volume flow rate
W_{sw}	Switching energy loss

Abbreviations

BJT	Bipolar Junction Transistor
Cu	Copper
DAQ	Data Acquisition System
DCC	Double Chamber Calorimeter
DIN	Deutsches Institut für Normung
DJC	Double Jacketed Calorimeter
DUT	Device Under Test
EMI	Electromagnetic Interference
FACTS	Flexible Alternating Current Transmission Systems
HVDC	High Voltage Direct Current
IGBT	Insulated gate bipolar transistor
MOSFET	Metal oxide semiconductor field effect transistor
PC	Personal Computer
PCB	Printed Circuit Board
PID	Proportional Integral Differential
Pt	Platinum
RPBE	Realistic Perturbation-Based Estimation
RSS	Root Sum Square
RTD	Resistance Temperature Device
TRIAC	Triode for Alternating Current
WCE	Worst Case Estimation

1 Introduction

1.1 Motivation

The focal point of the major research interest in electromechanics now lies in the estimation, analysis, optimization and reduction of power losses in the electric machines. In general, the power losses can be attributed to the design and constructional aspects of the rotor or stator, including the rotor or stator design, the material properties and also to the various operational losses. Also worth mentioning are the harmonic losses during the machine operation, which are due to the switching cycles of the power electronic devices in the electric drives and converter systems which govern the machine operation. With the ever growing global demand for electrical energy, the attention is now more than ever on renewable energy sources and developing extremely efficient devices and improving on existing systems to save on energy.

Power electronic converters and devices are a crucial part of the auxiliary systems at a power generation facility. The auxiliary systems encompass the drives, instrumentation, control and optimization systems whose purpose is to enhance the plant's output. The efficiency of the power generation thus rests also with the efficiency of the auxiliary systems. Around 70% of the world's power plants still rely on fossil fuels, biomass or solid waste to generate electrical energy. 7-15% of the power generated at fossil fuel plant is consumed by the plant's auxiliary systems. Intelligent converters with high efficiency, minimal wastage and higher power density is thus, the ideal that engineers are aiming to achieve. With the research and advancements in power electronic switches and their loss minimisation, this is a solution which is as technologically feasible as it is green.

1.2 Problem Statement

In general, the efficiency of power electronic devices is very high; around 90% - 95%. The power losses are attributed to eddy currents, hysteresis and skin or proximity effects. However, the theoretical and experimental quantification of these losses are rather difficult, especially at high switching frequencies [1]. The traditional electrical method of measuring the power losses of systems by finding the difference between input and output powers is largely erroneous, as discussed in [12]. In electric power measurement schemes, the phase-errors during measurement in the AC-systems and electromagnetic interference (EMI) of the switched-mode power supplies result in inaccurate measurements. Precise data on device power loss will aid the design process to create low-cost devices with improved thermal characteristics, overall performance and energy efficiency, as is the need of the day.

Calorimetry, as a technique for power loss measurement technique in electrical and electronic components, is gaining in popularity and is establishing itself as a viable method for the same. It only measures the total heat lost from the device and so neither is it measurand specific, nor is it affected by factors like power rating, supply distortion, which plagues the traditional input-output technique of power

loss measurement. High levels of accuracy are hence achievable with calorimetric power loss measurement techniques. This will further enable exact assessment of the performance of the device, thus paving way for development of improved designs.

1.3 Objectives

The objectives of this work are:

- To analyse the various calorimetric techniques available for measuring power losses.
- To design a calorimeter suited for our device which belongs to a power class of under 1 kW.
- To achieve power loss measurement accuracy better than 0.5%.

1.4 Thesis Structure

This section outlines briefly, the basic organisation of the thesis report.

Chapter 2 : Background literature study of the various power losses in power electronic devices in general and frequency converters in particular.

Chapter 3 : Calorimeters and Related work. Study of the different existing designs of calorimeters and the methodologies undertaken so far in the research towards accurate measurement of electric power losses in power electronic converters.

Chapter 4 : Experimental setup of the calorimeter and the detailing of its construction, instrumentation, methods adopted in measurement and its implementation.

Chapter 5 : Measurement results from the balance test and actual tests.

Chapter 6 : Discussion of the obtained results and the conclusions drawn from the observations made. Suggestions for improvement in the future are also discussed.

2 Losses in Power Electronic Systems

The observed power losses in power electronic circuits occur in the power semiconductor devices, windings and cores of the magnetic components, capacitors subjected to high-ripple current and auxiliary circuits like gate-drives [2]. These components are an essential and indispensable part of the circuitry in all power electronic systems. Hence even the most robust and efficient devices tends to waste a considerable amount of power as heat during normal switching cycles. For this reason, aspects like losses, power handling and cooling schemes have become critical to the design process. Achieving a better understanding of the root causes of the power losses and its manifestation, will contribute towards a deeper study of the subject of loss analysis, estimation, measurement and optimisation. The various losses in power electronic circuits are many and have been discussed further on.

2.1 Conduction Losses

On-state conduction losses also known as (*static losses*) of the semiconductor devices like thyristors, diodes, BJTs contributes to over 90% of the total losses incurred by the power electronic device. Conduction losses depend on the voltage drop across the device when in ON-state and the current flowing through it. Ideally, a power device should be able to conduct arbitrarily large currents with zero voltage drop when turned on. And in practical devices, this net forward voltage drop translates to heat energy dissipated by the device. Static losses broadly refer to the copper losses: I^2R (heat) losses of the semiconductor components as well as those dissipated in the connection wires and PCB traces and in inductors, capacitance series equivalent resistances. Larger semiconductor devices exhibit lesser on-state resistance and hence lower conduction losses.

The conductors carrying current have a net resistance and cause DC copper losses of

$$P_{\text{cond}} = I^2R \ , \tag{2.1}$$

where I is the r.m.s current flowing through the wire and R is the resistance

$$R = \rho\frac{l}{A} \ . \tag{2.2}$$

Here, A is the cross-sectional area of the wire, l is the length of the wire and ρ is the resistivity of the wire material.

2.2 Switching Losses

Switching loss (also known as dynamic loss) as the name suggests, refers to the power lost when the power semiconductor device transitions from the conducting to the non-conducting state and back. It mostly consists of the turn-on and turn-off switching losses and switch transition losses. These losses result due to the fact that voltage and current flowing through semiconductor switches do not change instantaneously.

There are various losses which contribute to the switching power losses: power loss caused by the output and junction capacitances as well as parasitic inductances of power diodes and power switches (MOSFETs, IGBTs, etc), the reverse recovery energy in p-n junction diodes and the leakage inductances of the transformers [4]. High voltage and current fluctuations during transients also lead to high dynamic power losses. Switching losses lead to heating, thus raising the junction temperature of the switches.

The switching losses vary proportionally with the switching frequency and the values of parasitic capacitances. So on one hand, if larger switches mean lower conduction losses, on the other hand, it also implies larger parasitic capacitances and hence larger switching losses. And even though using fast switching devices can minimize the energy lost in the on-off transitions and reduce acoustic noise, it will cause higher internal losses giving rise to radiated electromagnetic interference. At high switching frequencies, the switching losses are even higher than the conduction losses. The design challenge is thus to achieve a balance between the conduction and switching losses.

If W_{sw} is the total energy lost in all the switching transitions and f_{sw} is the switching frequency, average switching power losses P_{sw} is

$$P_{\text{sw}} = W_{\text{sw}} f_{\text{sw}}. \tag{2.3}$$

The figure below illustrates how the switching frequency at an operation point is limited by the junction temperature.

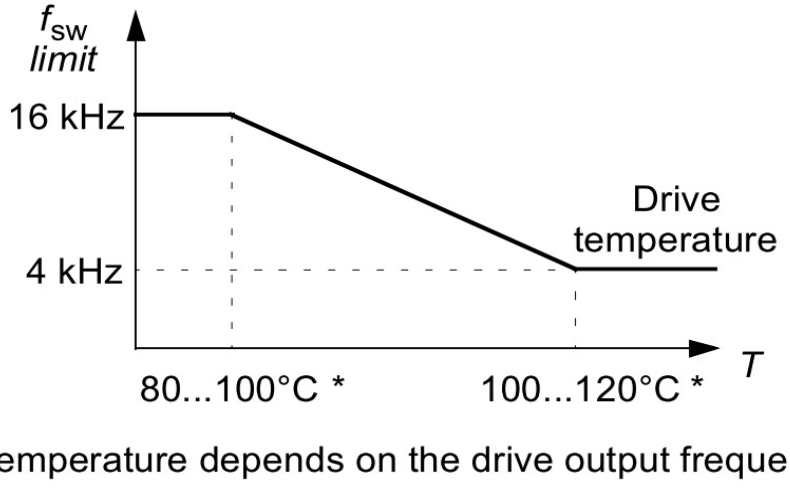

Figure 2.1: Switching frequency vs. junction temperature. Figure from ABB-Drives-ACS350-User-Manual.

2.3 Losses in Magnetic Components

In the power electronic circuits and systems are present, many magnetic components such as filter inductors, multi-winding coupled inductors, deflection coils and

Extreme High Tension transformers, saturable reactors and such, the magnetic cores of which exhibit hysteresis and saturation. These components are vital to a system in carrying out functions of amplification, filtering, isolation and aiding in resonant transitions in some circuits.

2.3.1 Eddy Current Losses

Magnetic materials are fairly good conductors of electricity. When they are subjected to high-frequency magnetic fields, circulating currents or eddy currents are induced in them as per the Lenz's law. These induced currents flow in paths to oppose changes in the core flux and hence in effect, prevent flux-penetration of the core. At high switching frequencies, the magnetic core and windings of the inductors and transformers in the power electronic circuits are very susceptible to this phenomenon which is responsible for considerable power loss in these devices. Eddy currents can also be caused due to radiation of AC electromagnetic fields from the equipment. Classical Eddy current power losses are categorised as core loss.

Eddy currents in winding conductors cause two effects, namely:

Skin effect: Caused due to opposing eddy-currents. As the frequency increases, the skin depth decreases, thus reducing the effective cross-sectional area of the conductor. As a result, the current flow is concentrated only on the surface of the conductors, thereby increasing the resistance, as can been seen from equation (2.2).

Proximity effect: Another related effect wherein eddy currents are induced in a conductor (of thickness equalling or greater than the skin depth) by the AC current flowing in the adjacent conductor. This phenomenon causes significant copper loss at high frequencies to the windings of high-frequency transformers and AC inductors, hence leading to undesirable heating. PWM (Pulse Width Modulated) waveform harmonics also contribute to increased proximity losses.

2.3.2 Hysteresis Losses

In the ferromagnetic core of the inductors and transformers, due to magnetization and subsequent relaxation, hysteresis losses are generated. Magnetic hysteresis losses also increase with increase in frequency.

2.4 Summary

The high efficiency of power electronic systems is achieved thanks to the fact that the entire circuitry is majorly made of semiconductor switches and energy storage devices that ideally do not dissipate energy. The goal of the industries has been product compactness and miniaturisation. Hence smaller passive components are much sought after. Smaller components respond faster to load changes and thus exhibit improved transient performance. And although high (switching) frequency operation enables use of smaller components, considerable copper losses as well as magnetic core losses would be incurred thus, resulting in heat. Increased temperatures lead to increased on-state resistance, further leading to power losses which may

even cause component failure. In high power semiconductors, to limit the junction temperature from rising, specialized heat sinks or active cooling systems are used.

The converter's total losses can be expressed as

$$P_{\text{loss}} = P_{\text{cond}} + P_{\text{fix}} + P_{\text{sw}} \tag{2.4}$$

where

$$\begin{aligned} P_{\text{cond}} &= \text{Conduction Losses} \\ P_{\text{fix}} &= \text{Fixed Losses or core losses} \\ P_{\text{sw}} &= \text{Switching Losses.} \end{aligned}$$

Choosing a suitable flux density and appropriate core material, and employing suitable air-gaps helps mitigate the electromagnetic power losses. Saturation can be prevented by increasing core cross-sectional area or increasing the number of primary turns.

The figure below illustrates the relationship between converter efficiency and switching frequency. The maximum achievable frequency of the power converter is at switching frequency called critical frequency $f_{\text{crit}} = \dfrac{P_{\text{cond}} + P_{\text{fix}}}{W_{\text{sw}}}$. If this limit is exceeded, the efficiency drops rapidly with the frequency. So, the power loss sustained in each switching cycle singularly restricts the frequency of operation of the power converter.

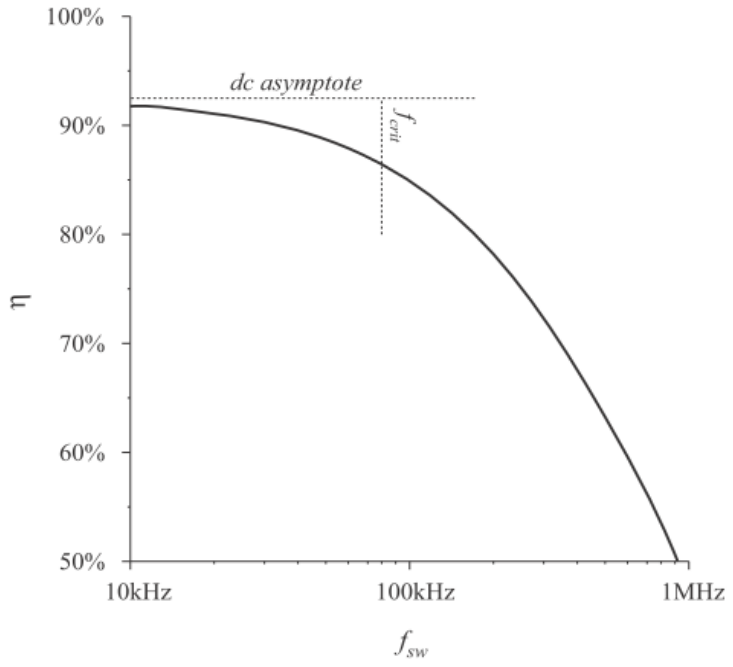

Figure 2.2: Converter efficiency vs. switching frequency [3].

3 Power Loss Measurement Techniques

3.1 Overview

Quantitative knowledge of power loss of electrical devices goes a long way in aiding the understanding of the device's operation, identification of major causes of losses and its propagation mechanisms and providing relevant markers for future design processes for device optimisation. In electric machinery, the dominant methods of loss analysis and quantification are namely the: Input-Output Method, Segregated Loss Method, Calorimetric Method.

In high-power electric machines, the power losses are large and the conventional input-output method (which follows the basic definition of power loss $P_{\text{loss}} = P_{\text{out}} - P_{\text{in}}$) gives satisfactory results. But in systems with low losses, this method is no longer considered reliable as it is restricted by high machine efficiency and measuring instrument accuracy. Additionally, the error caused by the difference method results in considerable overestimation of measurement error [6], [15]. The segregated loss method proceeds by measuring each loss component through specifically designed tests. The stray loss component's quantification however, remained elusive in this method. The calorimetric method, on the other hand, has been adopted for electric loss measurement in different variations for various electric motors as well as power transformer with much success in [5]-[10]. It has also been adapted for segregated loss measurement of machine stator losses and stray losses in [8] and [11] respectively.

3.2 Power Loss Measurement in Power Electronics

With power electronic converters and systems, it is a different ball game altogether. The research in power electronics is striving to make the converters more compact to achieve higher efficiencies with higher power densities at higher switching frequencies. But as discussed in the previous section, these credentials are that which spell complex loss mechanisms and greater device heating. To enable proper power handling, better techniques of loss quantification are needed, which can effectively validate the loss model predicted from simulated runs. The various power loss measurement techniques applied to power electronics are discussed further on.

1. **Electrical Methods**

   Power calculations are done by obtaining the product of the measured voltage drop and current flowing through the device. These measurements are achieved through:

   (a) **Analog Measurement Techniques**

   Analog measuring instruments like watt-meter, voltmeters and ammeters are used to measure the electrical quantities in DC as well as low frequency analog circuits.

   (b) **Digital Measurement Techniques**

Digital instruments like oscilloscopes are suitable for, and are widely used in circuits with high frequency signals and harmonics as in a typical power electronic system. These instruments digitally acquire the instantaneous current and voltage values, subsequently simultaneously samples them, and then finds their averaged product to give the power value.

Input-Output Method This classical method discussed earlier can be extended to power converters. The difference between input and output power values measured by a power analyzer gives the power loss of the converter. Efficiency is calculated as,

$$\eta = \frac{P_{\text{out}}}{P_{\text{in}}}.$$

$$\text{And, } P_{\text{loss}} = P_{\text{in}} - P_{\text{out}} \Rightarrow P_{\text{loss}} = \frac{P_{\text{out}}}{\eta} - \eta P_{\text{in}}.$$

The maximum relative error in loss measurement can be expressed as,

$$\left|\frac{\Delta P_{\text{loss}}}{P_{\text{loss}}}\right| < \frac{1}{1-\eta}\left(\left|\frac{\Delta P_{\text{in}}}{P_{\text{in}}}\right| + \left|\frac{\Delta P_{\text{out}}}{P_{\text{out}}}\right|\right).$$

Now, for a highly efficient converter with η =95% and relative error in measurement of the input and output powers 1%, the relative error on loss measurements is 31 times greater than the relative error given by the measurement device. So, the relative error from differencing is much greater than the initial error, especially for highly efficient converters.

Component Power Measurements are also done with digital devices. The switching losses of semiconductor power switches and core losses of the magnetic components [18] can be measured separately. However, due to the huge voltage dynamics between the ON and OFF states of the switches, there is difficulty measuring conduction losses. Also, in high-frequency magnetic cores, the ground lead and the measuring probe input capacitances may induce high-frequency resonance, thus damaging the measurement accuracy. In such setups, Common mode noise and EMI are other causes of concern.

Opposition Method described in [22], measures the power losses directly so that the relative error depends solely on the accuracy of the measuring device and not on the efficiency of the tested device;

$$\frac{\Delta P_{\text{loss}}}{P_{\text{loss}}} = \frac{\Delta P}{P}$$

thus achieving high accuracy in measurement of total losses.

It involves operating two identical and reversible (w.r.t.energy flow) systems together, one as a generator and the other as a receptor, with their

control schemes synchronised. This way, the power is circulated within the system and the power drawn from the supply is only to satisfy its intrinsic power losses. Thanks to this, the load inductor value is considerably reduced, and the losses in passive components are negligibly diminished. Another plus of this method is that it enables loss analysis of the converter in different operating modes. On the flip side, this method can't be applied to converters which cannot operate reversibly, for e.g. diode rectifiers. Moreover, even though the systems are identical, since the generator and receptor modes of operation are different, the operation conditions have to be carefully chosen so as to somehow balance the losses symmetrically between the two systems.

2. **Thermal Method**

   Thermal or calorimetric method measures the heat dissipated by the system and uses that as a direct measure of the power lost during the system operation. The coolant temperature difference is taken as the indicator of the heat dissipation, provided the coolant's fluid and thermal properties remain constant. It is an accurate alternative to the other methods discussed before, which were either too erroneous or unsuitable for some systems.

A large quantity of published work [12]-[21] deal with calorimetric techniques in power electronics and they all have reported high measurement accuracy and reliability. This work too will discuss the calorimetric method in general as well as in detail and undertake a brief study of this technology as applied to power electronics.

3.3 Calorimetry

Calorimetry is the underlying principle of the calorimetric power loss measurement technique. Calorimetry, as its name implies, (*'calor'* in Latin means heat) simply refers to the measurement of quantities of heat. Primarily applied in the field of chemistry, calorimeters are used to measure the heat generated by (enthalpy of) a chemical reaction, in order to find calorific values and specific heat capacities of test substances.

3.3.1 Principle of Operation

The power losses in all machines appear as dissipated heat. So, true to the law of conservation of energy, the power losses can be measured by measuring its effect- heating of the machine and the surrounding medium through the processes of conduction, convection and radiation.

Calorimetric methods are many and could broadly be any of these four: Drop calorimetry where the Device Under Test (DUT) is immersed in a chamber filled with the cooling fluid, or flow calorimetry which relies on the input-output temperature difference of fluid in a flow channel cooling the DUT, heat flow calorimetry which determines heat flow based on the Seebeck Effect and bomb calorimetry which is

used to measure the heat of combustion of a chemical reaction to ascertain the calorific content of a fuel.

The principle of Flow calorimetry is the one of interest in this work. The machine to be tested is placed inside a hermetically sealed chamber called the **calorimeter**. The medium/coolant (air, water or other coolant) to which the heat is transferred, is controlled and its thermal and flow properties are measurable and known.

The heat generated by the DUT or heat transferred to the cooling fluid from the DUT during the calorimetric process, Q is given by the equation

$$Q = m \cdot c_p \cdot \Delta T \tag{3.1}$$

where, mass is volume times density: $m = V \cdot \rho$ and c_p is the specific heat capacity of the coolant and ΔT is the change in coolant temperature. Power is the rate of change of energy. Assuming the c_p, m and ΔT remain constant, the rate of heat-transfer ($\dot{Q}$) from the DUT to the cooling fluid, is the same as the electrical power P_{loss} lost from the DUT. That is,

$$P_{\text{loss}} = \dot{V} \cdot \rho \cdot c_p \cdot \Delta T = P_{\text{water}}, \tag{3.2}$$

where $\dot{V}$ is its volume flow rate of the cooling fluid for e.g. water and P_{water} is the power absorbed by water.

Provided that the heat generated is substantial enough to raise the temperature of the medium surrounding the machine from the ambient, the principle of calorimetry is one ideally suited for accurate direct measurement of electrical losses of tricky systems: inductive circuits, circuits operating at high frequencies as well as machines supplied by power converters.

3.4 Types of Calorimeter

Calorimeters, based on their design and coolant types can be classified into different types. The process of estimation of electric losses from a calorimetric measurement are also explained in brief.

3.4.1 Based on Heat Exchange Mechanism

The choice of the cooling medium in the calorimeter decides its structure also. Calorimeters can either be :

• **Gas-cooled Open-type Calorimeter**: It is the most simple in design and construction and uses air as the coolant. The calorimeter is of the 'open' type as the air pipes or vents built into the calorimeter structure facilitate **direct** heat exchange to the air outside. However, the difficulty with an air-cooled system is that the physical and thermal properties like humidity, pressure, density etc. of air are never constant over a period of time. The hugely fluctuating tendencies of these properties make the accurate estimation of losses very complicated. Also, since the specific heat capacity of air is lower than that of liquids, to transfer the same amount of power, the volume of air required is more. Hence the air-cooled mechanisms tend to be much bigger in dimensions.

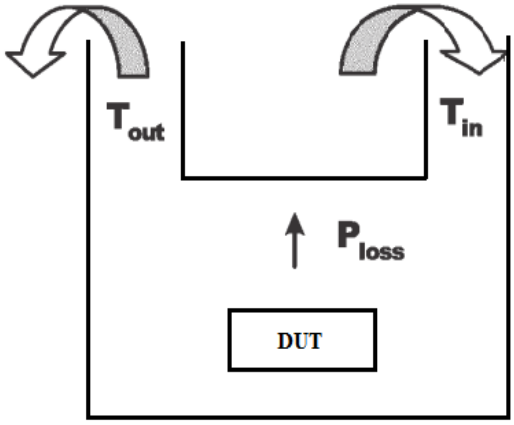

Figure 3.1: Schematic of an open, air-cooled calorimeter.

• **Liquid-cooled Closed-type Calorimeter**: This calorimeter uses a liquid coolant-commonly water and mostly uses an air to water heat exchanger to absorb the heat dissipated inside the chamber. Since water is circulated in closed channels around the calorimeter, the calorimeter becomes of the 'closed type'. Actually the water cools the DUT only **indirectly**, by absorbing the heat content of the warmer air around the DUT. Still, the accuracy of this type of calorimeter is better than the gas-cooled open-type's. This is because liquids have higher density, heat capacity and thermal conductivity than gases. Also, the thermal properties of water are greatly more consistent across a temperature range over a period of time, as compared to that of air.

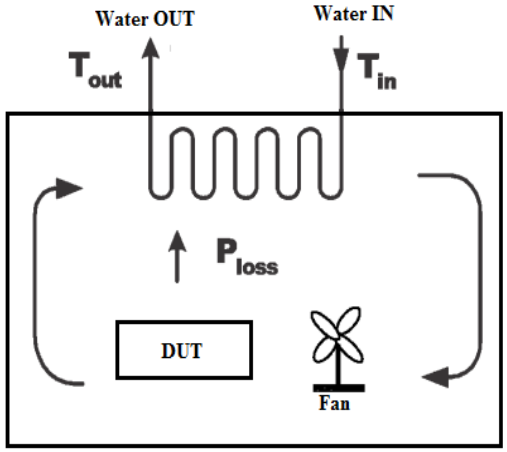

Figure 3.2: Schematic of a closed, water-cooled calorimeter with fan and heat-exchanger.

3.4.2 Based on Design

• **Balanced Calorimeter**: Turner *et al.* [5] used a single chamber balanced open type calorimeter for testing squirrel cage induction motors. It operates by carrying out two similar tests. First test was conducted with the actual machine and the stable air temperature was recorded. Then the test machine is replaced with a heater or resistors supplied by a known power source so as to achieve the same air temperature rise as that achieved previously. Assuming the coolant flow and heat leakage conditions are consistent in both tests, the power supplied to the heater in the second test equals the power lost by the DUT in the first. With this technique, there is no more the need to accurately ascertain the coolant's thermal properties like in open-type calorimeter tests. But, for the power drawn by the resistors to be considered equal to the power lost by the machine, the air flow and thermal conditions have to be kept constant as in the actual machine test, which is indeed very difficult.

• **Series/Double Chamber Calorimeter**: Proposed by Jalilian *et al.* [7], the double chamber calorimeter(DCC) is an improvement to the balanced calorimeter and presented an arrangement for both the tests to be carried out simultaneously. As is evident from its name, the series calorimeter has two consecutive chambers, identical in all respects, first one for the actual test device and the other one for carrying out the balanced test. The coolant flows from the first chamber to the second. Even though this method cuts the test-time by half; on the downside, it may give inaccurately high power-loss readings [1]. This is because, since the same temperature rise has to be maintained, the coolant is hotter in the second chamber than in the first leading to greater heat leakages. Also, the thermal properties of the coolant can change with the increased temperature level in second chamber. Owing to the larger volume required for this calorimeter design, the construction costs are higher.

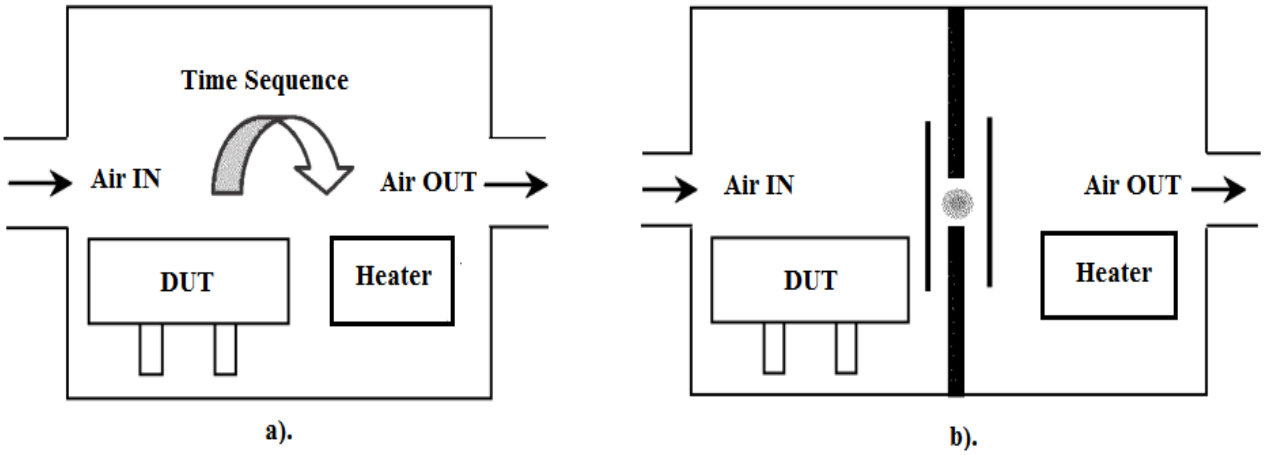

Figure 3.3: a). Single chamber balanced calorimeter b). DCC or the series calorimeter [23].

• **Double Jacketed Closed-Type Calorimeter**: This calorimeter was proposed by Malliband *et al.* in 1998 for measurement of electric machine losses, and was later extended to power inverters as well [14]. The Double Jacketed Calorimeter (DJC) uses water as the secondary coolant and to ensure zero heat leakage, there is an additional thermally insulated chamber concentrically within a larger one, separated by an air gap. The idea is to control the temperature of the air-gap T_e to match the temperature inside the inner chamber T_i where the DUT is placed. Since heat only flows when there is a temperature difference, the idea is to eliminate any such gradient over the inner and outer surfaces of the chamber walls, thus ensuring zero leakage. Wall heat leakage is highly undesirable especially while measuring for highly efficient converters. The power lost through the chamber walls should be less than the accuracy P_{acc} required from the calorimeter. This way it can be ensured that all of the device losses are absorbed by the coolant which is circulated in the inner chamber. As opposed to the DCC, this calorimeter is much more accurate and has significantly less measurement time. The air-gap temperature control is governed by the relation $|T_i - T_e| < P_{acc} R_{th(in)}$, where $R_{th(in)}$ is the thermal resistance of the inner walls.

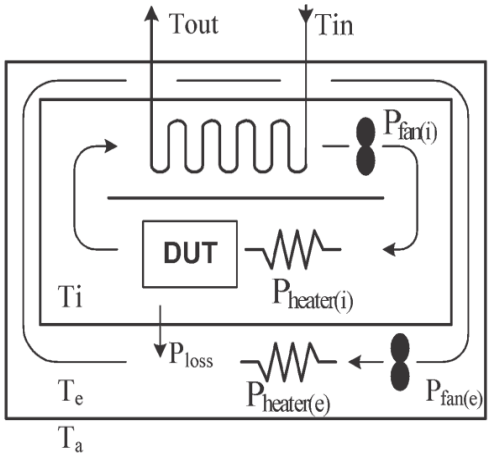

Figure 3.4: Schematic of double-jacketed, closed type calorimeter [18].

3.5 Overview of Related Research

While Calorimetry with the double jacketed design is becoming an increasingly popular technique to study losses of high-accuracy devices like power electronic converters as seen from literature [12]-[15]; the open-type air-cooled calorimeter is the one favoured for test with high-power rated induction or synchronous machines [9]. Jalilian *et al.* in [7] illustrated the application of a DCC to measure the harmonic losses of a 7.5 kW cage induction motor and contrasted this method's superiority over the single chamber type calorimeter.

Blaabjerg *et al.* first proposed the double jacketed construction in [15] with active air-gap temperature control, achieving accuracy of 0.2% for power losses of 50 W. Malliband *et al.* [14] improvised further to fully automate the DJC, achieving

measurement accuracy ±0.5 W for losses of 200 W. Electronic ballasts of CFLs and phone chargers where also tested with the DJC by Weier *et al.* in [13] to successfully ascertain their losses to an accuracy of ± 0.1 W for 25 W power loss. This paper notes that since the copper plates on the outer wall of the inner chamber keep its temperature constant, the air gap can be done away with, returning the calorimeter to a more compact single chamber structure. Christen *et al.* (2010) in [12] realized ±0.4 W or 1% accuracy in measuring losses of 10 W-100 W for power electronic systems with full range power between 1 kW-10 kW, also with a Closed DJC. In all the papers, the coolant flow rate has been controlled with a flow sensor and a pump control loop, and a common observation has been that the inlet water temperature fluctuations result in reduced measurement accuracy at lower power levels.

Bomb Calorimetry[18]: A complex measurement setup has been used in [19], where Bomb calorimetry has been applied. The device tested is a small power converter placed in oil in a Pyrex Glass container along with a mechanical agitator, calibration resistance and temperature sensor. The agitator ensures uniform and faster heat diffusion throughout the oil coolant. The glass container is itself placed inside a metal can, with a lid to support the agitator shaft. This setup is secured tight with a waterproof cover and is then placed inside a larger isothermal water tub. This method also follows the basic calorimetric principle followed in others, but relies on the thermal capacity, rather than on the flow rates of the coolant. Construction of this calorimeter is complex and expensive as well.

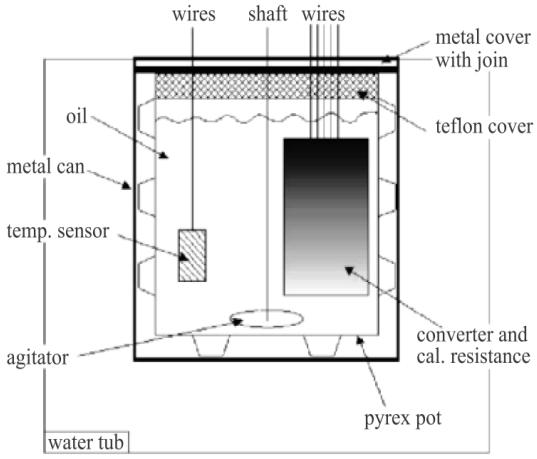

Figure 3.5: Schematic of calorimeter implemented by Ammous et.al. in [19].

Calorimetry using heat flux sensor: The effectiveness of this calorimetric technique requires "the heat from the dissipating device to escape to the environment via a fixed, predefined heat flow path"[25]. In this technique applied by Sridhar *et al.*(1999), the DUT is mounted on an chilled liquid-cooled aluminium base plate serving as the heat exchanger. On this plate is placed a heat flux sensor to sense the total heat generated by the DUT. The whole setup is enclosed in a evacuated chamber with polished inner walls. Accuracy of ± 5% is achieved. Precision of results depend on how well the heat from the DUT can be ensured to flow through the base into the heat flux sensor which will produce a steady state voltage output. This

limits the applicability of this method to relatively small planar components. But since it doesn't need regulated fluid flow systems, it is simple to construct, easier to implement and time constants are also less.

In [26], Chen *et al.* have implemented a calorimeter with a heat-flux sensor inspired by the design of double jacketed calorimeter. Reduction in heat leakage was achieved by minimising the temperature gradient between the polished inner and outer aluminium covers of the calorimeter chamber, through suitable temperature control with thermoelectric (TE) modules. The measurement apparatus was tested with an Integrated Power Electronics Module (IPEM) and accuracies better than ± 5% were achieved for power losses of 50 W. The calorimeter is small in size and well suited for low-power loss measurements.

A low-cost calorimeter for measuring losses in the range of 1 W-30 W was developed by Dimitrakakis *et al.* in 2011 with a Dewar vessel (used for storing liquefied gases at very low temperatures) as the calorimetric tank, which holds the DUT immersed in the calorimetric fluid - transformer oil. It is a reliable method for loss measurement of power electronic components like high frequency magnetics and semiconductor switches.

Extremely low measuring times characterises the calorimetric watt-meter presented by Kuebrich *et al.* in [27]. The transient temperature rise of power semiconductor components is determined in order to obtain their power losses accurately. Since there is no need to reach thermal equilibrium in this measurement process, the measurement time is under 1 min. This is very fast for usual calorimetric methods, which have huge time constants.

3.6 Summary

While measuring small power losses as in case of highly efficient power converters, the heat leakage through walls can be very undesirable indeed. If thicker walls are used to counter the leakage, it will result in larger settling or response time of the calorimetric process. Although the setup and control schema maybe complex, the DJC with active control of the test chamber wall surface temperature addressed these issues effectively.

Calorimeters suitable for different devices of different sizes and power classes are being developed based on various principles and quite innovatively, like the Dewar vessel calorimeter. Maximum reported accuracy of closed calorimetric systems is 0.2% for powers of 600 W – 1.5 kW.

The aim of the work is to devise a simple calorimeter for power losses ranging from few tens to couple of hundreds of watts with an accuracy of 0.5%. These requirements are yet to be tested with a regular closed, single chambered, single walled, water cooled calorimeter. The endeavour of this experiment undertaken is to attempt to successfully do so, with favourable results.

4 Calorimeter Experimental Setup

The device to be calorimetrically tested is a frequency converter with output power of 0.75 kW. According to its specification sheet, the efficiency is of 95-98% at nominal power level. Hence we can safely consider the device to have an average operating efficiency of around 90%, which means the power losses amount to around 75 W. But chances are that the actual efficiency of the converter maybe lower, even 85%.

Whichever the case, the electrical power dissipated as heat from the converter are considered to vary up to a maximum of around 100 W , which will then be measured accurately with the rise in temperature of water in the radiator. If 75 W of power is lost as heat, it will result in water temperature rise of about 5℃, with the inlet water temperature at 15℃. Hence, as per equation (3.2), for 75 W power loss ($\eta = 90\%$),

$$\dot{V}_{\text{water}} = 215.59 \text{ ml/min} \approx 220 \text{ ml/min}. \tag{4.1}$$

If the ambient air-temperature is taken to be around 23℃, it is assumed that the heat dissipation from the DUT raises the air temperature inside calorimeter to around 30-31℃. Ideally, air which is the primary coolant must give up all of the heat it gained from the DUT to the cooler fluid- water which is the secondary coolant. So the equation (3.2) can be written w.r.t to air and water material properties as

$$\dot{Q}_{\text{air}} = \dot{Q}_{\text{water}}$$

$$\dot{V}_{\text{air}} \cdot \rho_{\text{air}} \cdot c_{\text{p,air}} \cdot \Delta T_{\text{air}} = \dot{V}_{\text{water}} \cdot \rho_{\text{water}} \cdot c_{\text{p,water}} \cdot \Delta T_{\text{water}}. \tag{4.2}$$

The temperature rise of the coolants and the heat exchanger 'effectiveness' (performance indicator of radiators analogous to 'efficiency') are interrelated. After considerations of the maximum allowable air-temperature rise inside the calorimeter, and the maximum temperature rise of water possible at the upper-limit of flow, a reasonable effectiveness of the radiator could still be achieved at different power levels.

4.1 Design

Analysing the pros and cons of the generic as well as specialized calorimetric design, a single chamber, closed, liquid-cooled design of the calorimeter for the purpose of loss measurement of frequency converter was decided upon. The aim of the design was to create a versatile calorimeter box which can be used for measurements with different kinds of small-sized power converter devices and other electrical equipments. Care was taken to reduce metallic parts inside the box as much as possible to reduce eddy current losses. Another concern was to provide good degree of thermal insulation to prevent leakage of heat energy, at the same time minimizing the time constant of the measurement system to reach steady state.

This calorimeter has two shells:

1. The inner calorimetric shell (100 cm × 80 cm × 60 cm) with its top open.

2. The outer shell (120 cm × 100 cm × 60 cm.) acting as the lid to the inner calorimeter box.

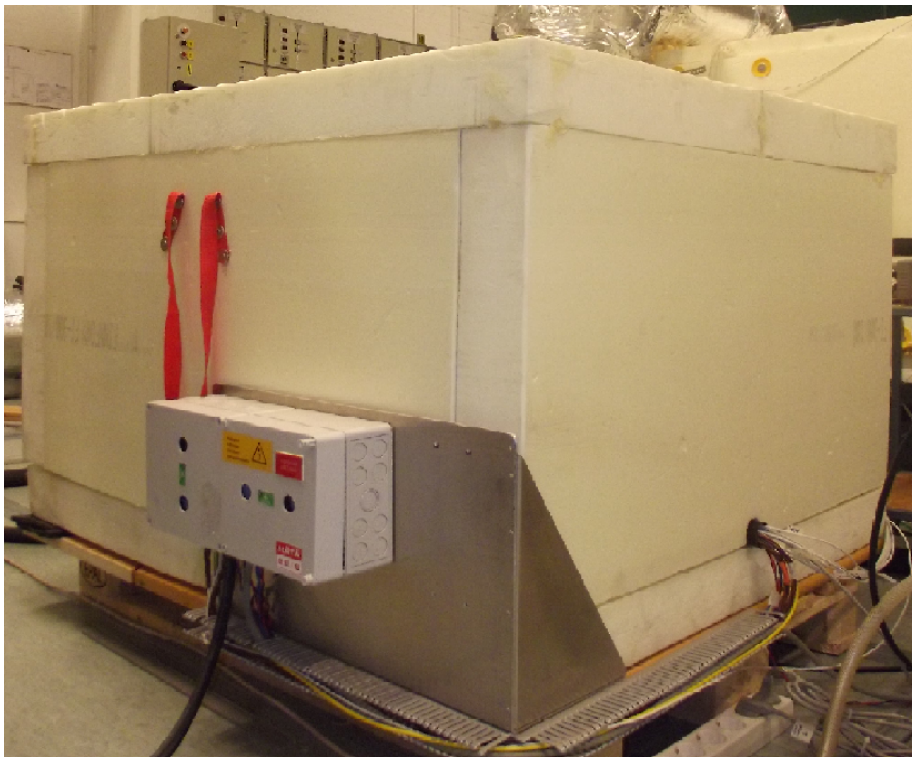

Figure 4.1: The calorimeter.

Both the shells are made from Finnfoam® extrusion-compressed polystyrene sheets of 10 cm thickness. The outer box is dimensioned so as to just fit over the inner chamber, leaving very little gap between the walls. It covers the inner shell completely. Where the shell edges touch, Armaflex® thermal insulation by Armacell was stuck, so as to ensure a secure fit with no leakages. Since the outer shell can be lifted off the top easily, it gives a better way (than seeing through a door) to check the layout of the component equipments in the chamber and making it easier to fix sensors, if need be. All the electrical connections, sensor wiring and water channels go through two separate tunnel tubes drilled in opposite walls, as can be seen from Figure 4.1.

[12] discusses the choice of wall thickness to be an iterative process of the design algorithm; especially if low settling time is an important design objective. The choice of the wall thickness is dependent on two aspects:

- Short settling time
- Minimum heat leakage through walls.

This calorimeter here has double sheathed insulation along the walls. The choice of a higher wall thickness was made singularly to minimise leakage, based on previous experience with the insulation material. The double shell structure resulted from the fixed thickness of the insulation sheets available in the market.

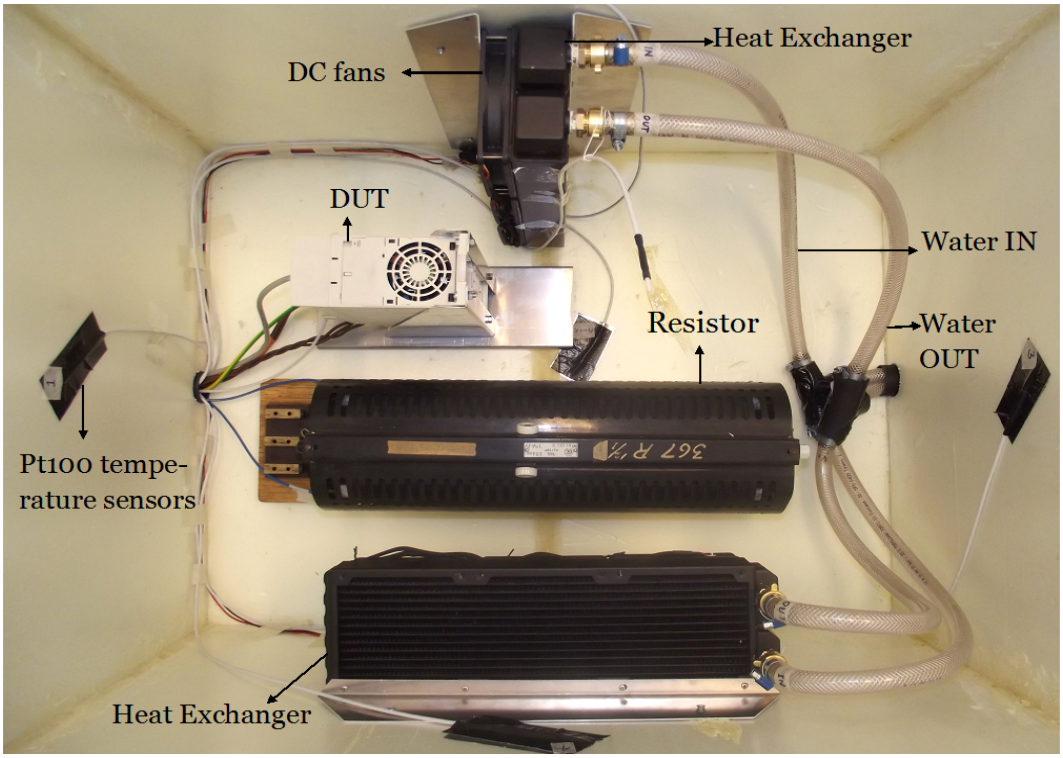

Figure 4.2: Layout of the calorimeter chamber.

Thermal Resistance

The four walls surrounding the DUT are double insulated by overlapping 10 cm thick slabs belonging to each shell, whereas the bottom as well as the roof has a single slab insulation of 10 cm. So, even though the material properties may remain constant owing to the uniformity of the polystyrene insulation, the thermal resistance it offers is anisotropic due to the variation in insulation dimensions in different directions. The thermal resistance is expressed by the equation

$$R_{\mathrm{th}} = \frac{d_{\mathrm{wall}}}{\lambda \cdot A_{\mathrm{wall}}} \tag{4.3}$$

where, R_{th} is the thermal resistance of the insulation, d_{wall} is its thickness, λ is the thermal conductivity of the insulation material: 0.05 W/(m·K) and A_{wall} is the area of the insulation slab surface in the calorimetric chamber. Hence, depending upon the wall thickness and the insulation slab dimensions, the heat flux from the DUT faces different thermal resistances, as presented in Table 4.1.

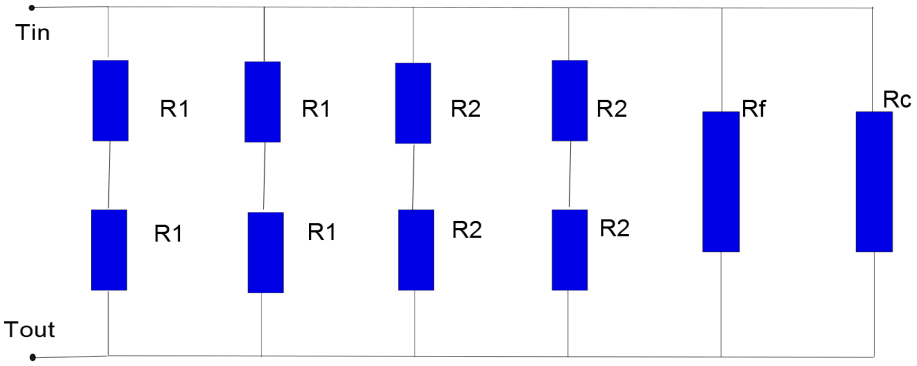

Figure 4.3: Thermal network of the calorimeter.

Here, $R1$ and $R2$ are thermal resistances of the walls of the calorimetric chamber and Rf and Rc are the thermal resistances of the floor and ceiling of the calorimeter box respectively. $T\text{in} - T\text{out}$ is the average temperature difference across the calorimeter walls. In this calculation to find the calorimeter equivalent thermal resistance, possible air-gaps between the two 10 cm thick slabs have been neglected.

Table 4.1: Wall thermal resistance.

Type	**Dimensions**(m)	**Area** (m^2)	**Thickness** (m)	**Resistance**(K/W)
Type 1 (R1)	0.6×0.6	0.36	0.1	5.5556
Type 2 (R2)	0.8×0.6	0.48	0.1	4.1667
Floor, Ceiling (Rf,Rc)	0.8×0.6	0.48	0.1	4.1667
Equivalent thermal resistance				1.11

Calorimeter equivalent thermal resistance $= 1.11 \ \frac{\text{K}}{\text{W}}$.

Time constant of Calorimeter

The thermal time constant τ of the system indicates the rate at which temperature changes are reflected in the system. It is the product of the thermal capacitance and the thermal resistance,

$$\tau = C_{\text{th}} R_{\text{th}}.$$

The thermal capacitance C_{th} of a material is its specific heat capacity c_p multiplied by mass as expressed by the equation $C_{\text{th}} = c_p V \rho$ where V is the volume and ρ is the density of the material. It is thus evident that as the volume of insulation increases, it will result in a greater time constant, meaning that the changes in temperature will be slower.

For polystyrene, $c_p = 1.3 \ \frac{\text{kJ}}{\text{kg} \cdot \text{K}}$ and $\rho = 34 \ \frac{\text{kg}}{\text{m}^3}$, and its volume in the calorimeter is 0.216 m^3.

The time constant for the calorimeter system is $\tau \approx 3$ hours. This indicates that under static conditions, the measurement process when uninterrupted, will take a minimum of 3 hours to settle down.

4.2 Measurement System Implementation

The principal measurements in this experiment are those of water temperatures and water volume flow rate, and wall temperatures. The accuracy and repeatability of the measuring meters directly affect the reliability of the final results obtained. Since the quantities of temperature and flow rate to be measured are rather small, instrument inaccuracy can lead to considerable errors. It is hence vital to choose suitable and highly accurate meters and controllers. The various measuring devices and meters have been listed below.

Table 4.2: Measuring devices and accessories used.

Parameter	**Device Type**	**Meter/Sensor**	**Producer**	**Properties**
Water Flow Rate	Flow Controller	LFC 8718	Bürkert	Accuracy 0.5% F.S. Repeatability 0.5% F.S.
Water Temperature	Ceramic wire-wound RTD	Pt-100 1/10 Class B	SKS Group	4 wired. Accuracy: ±0.03 ℃
Air/Wall Temperature	Ceramic wire-wound RTD	Pt-100 1/3 Class B	SKS Group	4 wired. Accuracy: ±0.10 ℃
Air to water heat exchanger	Radiator	Airplex XT 360	Aqua Computer GmbH	Brass casing, lamellae made of copper
Air flow	DC fans	-	Aqua Computer GmbH	12 V, 5 fins
Water Pressure	Pressure Regulator	-	Gerhard Götze & Co.	Max. inlet pressure 25 bar.
Water Preheater	Heating cables	Deviflex™	DEVI	2m long, 40 W heating capacity
Temperature Control	Temperature Controller	Model T16	Redlion	PID Control
Power Regulation	TRIAC	FC11AL/2	United Automation	Integral 26A TRIAC

4.3 Control Schema

Two control schema are possible: inlet water temperature control or water temperature rise control. The first method proceeds by maintaining the temperature of the incoming water a constant, for a constant water flow rate. The water temperature rise can then vary according to the heat power being measured.

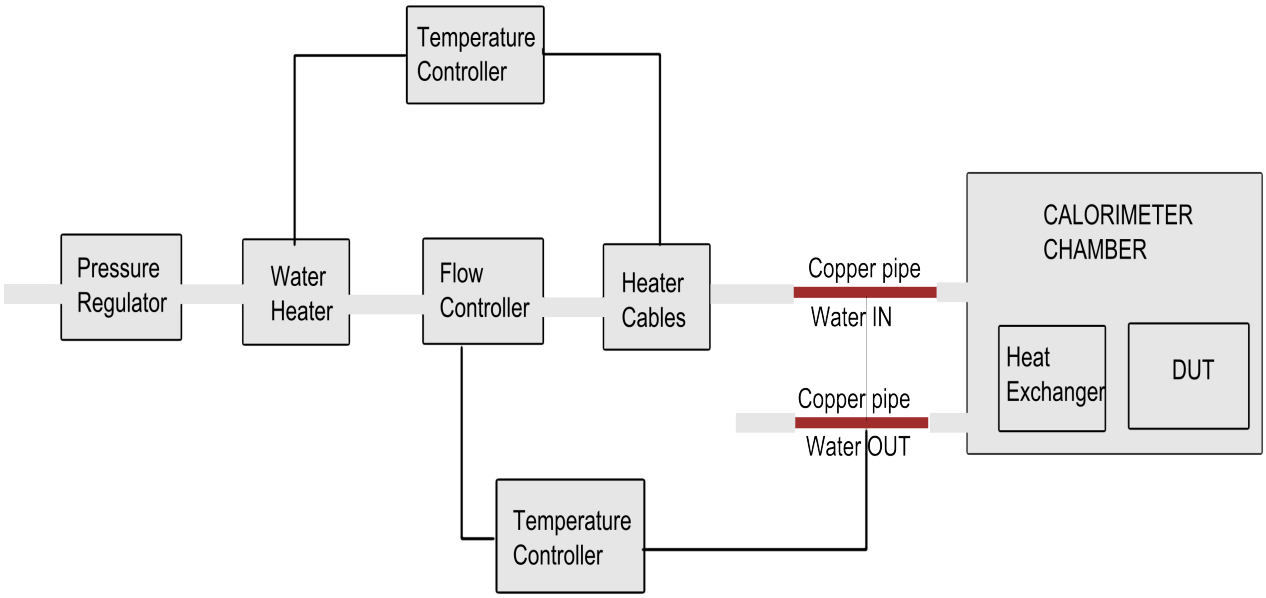

Figure 4.4: Block diagram of calorimetric system.

As an alternative to maintaining the a constant flow-rate throughout, a varying flow control mechanism can also be implemented. In this approach, the objective is to maintain the water temperature rise at a constant value throughout one measurement. If the rise in water temperature falls short of the expected, the PID control scheme generates control signals which communicate with the flow controller. Thus the water inlet water volume flow rate is regulated accordingly, to achieve the stipulated rise in temperature of the water passing through the calorimetric chamber.

The two control modes are illustrated in Figure 4.4. It is the first control sequence of inlet water temperature control that has been implemented in this work.

4.3.1 Flow Rate Control

The flow controller alone handles the volume flow control rate of the water coolant, and keeps it at a constant value, which is set when the experiment starts. The maximum flow rate that the controller can support is 300 ml/min. A pressure regulator was installed to maintain the water pressure around 3 bar, since the flow controller needs an input water pressure not exceeding 3 bar to function properly, as per its calibration.

4.3.2 Water Temperature Control

Usually, the thermal properties of water ensure that its temperature distribution across the water channels is more or less uniform. But, at different times of the day, normal tap water from the public distribution system may have fluctuating temperatures. If the temperature of the water being fed to the calorimeter keeps changing, it will affect the measurement stability and accuracy. Even if the water

heater unit which is acting like a water tank homogenizes the fluid temperature, persisting randomness due to the low flow-rate will make the water temperature measurements more prone to errors. So, a method to maintain the inlet water temperature a constant was devised.

This temperature control is achieved with a PID temperature controller and a TRIAC power controller. The power controller is mounted on a heat sink as per its operational requirements. The temperature and power controller combination exhibits good control performance. At very low flow rates, proper temperature control is even more challenging.

Water temperature measurement: The incoming and outgoing water of the calorimeter flows through short sections of copper piping right before it enters or leaves the calorimeter chamber. It is over these sections that, by measuring the surface temperature of copper, the temperature of the water flowing through it is obtained.

Ceramic wire-wound Pt-100 Class B 1/5 DIN, 4 wire sensors are used to measure the inlet and outlet water temperatures. Each RTD has two Pt-100 elements connected in series, 2 cm apart. Two such RTDs are plastered over the outer surface of a copper pipe, at different locations. The water temperature data from 4 different locations on the copper pipe is thus collected. The wire ends of these two RTDs when connected in parallel, gives the reading of the average water temperature.

Although silver is the metal with the best heat conductivity, due to cost considerations, copper was the material of choice for the piping carrying water. But these metallic pipes have been used to carry water only in those joints where the water temperature is being measured, and the measuring points are just outside the calorimeter. Everywhere else, plastic hosing has been used. The inlet water circuit to the calorimeter, including both the copper pipes are, covered with Armaflex® (an elastomeric thermal insulating shell), to counter the heat loss through the copper tubes.

4.4 Cooling Circuit

The cooling circuit of the closed water channels consists of two components: 1) the heat exchangers with the fans and 2) the temperature sensors with which we ascertain that the calorimeter chamber air is being cooled or not.

Temperature Sensors

Ceramic wire-wound RTD (Resistance Temperature Device) elements, such as the one used in this experiment were considered to incur more self-heating losses (the measuring current that flows through the sensor to generate the output signal, also heats up the sensor itself, thus causing the RTD to indicate a higher temperature result). Now with the recent advancements, the measuring current is so small that self-heating is no longer a problem.

RTDs belonging to class A have better tolerance than those of class B. However, the tolerances of the RTDs of different temperature classes are strictly valid only

for the temperature they are usually defined at: 0℃. For other temperatures, the tolerances follow their respective slope in the temperature vs. tolerance plot provided by the manufacturers. The slope can vary, depending upon the material the sensor is made of. The change in RTD resistance from its resistance at 0℃ (R_0) with temperature T is described by the Callendar-Van Dusen equation

$$R_{\mathrm{T}} = R_0[1 + AT + BT^2 + C(T - 100)T^3]$$

where

$$A = 3.9083 \times 10^{-3}\ \mathrm{K}^{-1}$$
$$B = -5.775 \times 10^{-7}\ \mathrm{K}^{-2}$$
$$C = 0 \ \text{ for } \ T > 0,\ C = -4.23225 \times 10^{-12}\ \ \mathrm{K}^{-4} \ \text{ for } \ T < 0.$$

The above equation was put to use to check the accuracy of the 4 sensor-scheme for the water temperature measurement described earlier. The total possible error in measurement with this arrangement of sensors was computed. Since the arrangement was in effect, a parallel arrangement of Pt 200Ω sensors, the uncertainty in measurement calculated coincided with the manufacturer data of the uncertainty of one single sensor. The relative error in case of resistance change with temperature was also less. So, a good averaged water temperature could hence be obtained without piling up additional measurement errors.

With reference to the above figure we see that even though Class B is of a lower grade than Class A, when it comes to tolerance, the tolerances of the improved Class B RTD's– 1/10 DIN, 1/5 DIN, 1/3 DIN are better than the Class A. Since temperature measurement range in question for the calorimetric experiment is rather small and since the expected temperatures achieved is low as well, possible departures from the tolerance slopes, if any, have been considered negligible and not taken into account.

In 2-wire RTD measurement circuits the lead wire resistance is read along with the resistance of the element. This problem of lead wire resistance is resolved with a 4-wire RTD, whose 4-wire circuit becomes a 4-wire bridge circuit that eliminates any differences in lead resistance electrically rather than to requiring to be fixed mathematically in post-processing of measured data.

Heat Exchange Mechanism

The air-water heat exchanger is a device crucial to this calorimeter's operation, since it involves the repeated heating and cooling of air by circulating water. The air to water heat exchanger Airplex XT 360 was chosen due to its suitable dimensioning. The heat exchanger was chosen keeping in mind the particulars of the procedure it was to be a part of. The maximum water and air-flow rates, the maximum measurement capacity of the calorimeter, as well as the thermal resistance of the heat exchanger are aspects which have to be considered in optimizing an appropriate heat exchange mechanism for the system.

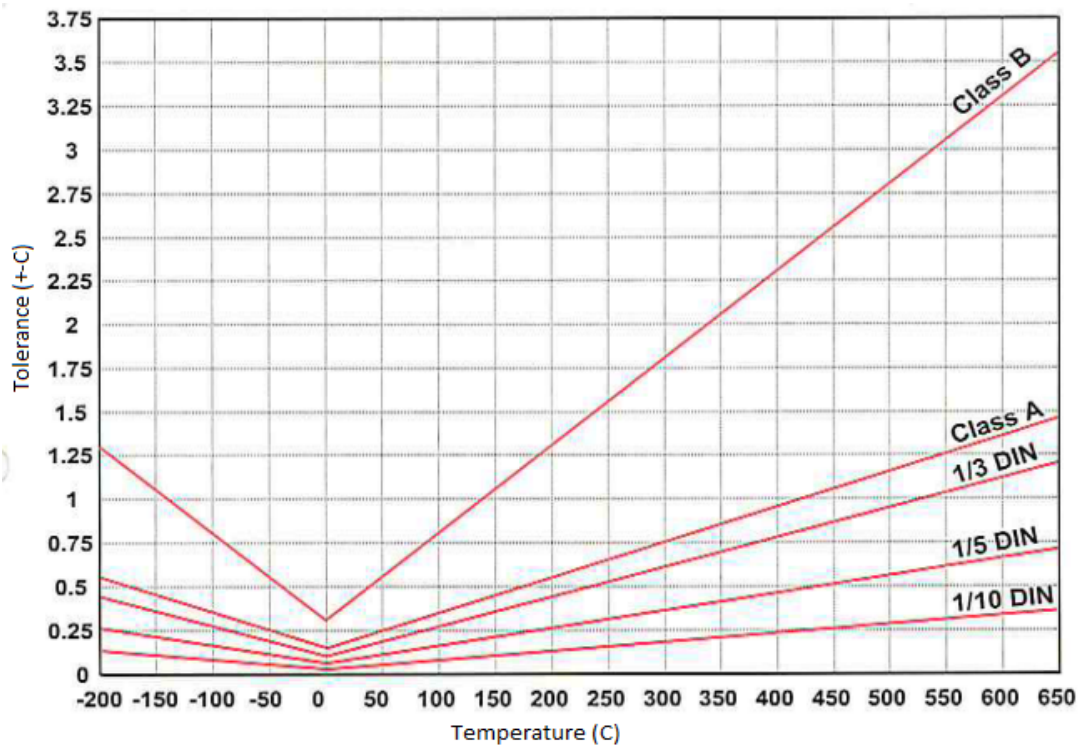

Figure 4.5: Tolerance vs. temperature plot of the Pt RTDs used (obtained from the manufacturer).

This is done with the help of the heat exchanger equations. Such an analysis is presented in Appendix A and helps in ensuring that the system performance remains stable, while the parameters stay within the limits. Accordingly, the maximum loss power that can be measured by the calorimeter was ascertained to be 520 W.

4.5 Power Measurement

Water flows at a controlled rate in the heat exchanger and absorbs all of the heat energy dissipated by the test device in the calorimeter chamber. In a perfect measurement all of the heat produced will be completely gained by the coolant. Thus the electrical power loss of the tested device will only be a function of the coolant temperature gradient at a fixed flow rate as described in equation (3.2).

This ideal calorimetric system is achieved with perfectly thermally insulating walls which ensure zero heat exchange to the outside. But a real calorimetric process is never adiabatic, and there will always be a certain amount of heat escaping through the walls. This heat leakage can be quantified and denoted as P_{wall}. If we also take into account the other non-idealities of the measurement system namely- the heat leakage through the copper wires present in the electrical connections inside the chamber P_{cu}, the heat generated by the air-circulation fans P_{fan} and other non-quantifiable losses P_{stray}, the power balance equation for the calorimetric system is redefined as

$$P_{\text{loss}} = P_{\text{w}} + P_{\text{wall}} \pm P_{\text{cu}} + P_{\text{stray}} - P_{\text{fan}}. \tag{4.4}$$

Wall Heat Leakage Loss

The walls are plane, without heat generation, constant surface temperatures and one dimensional temperature gradient. Analogous to the relationship between electrical current and resistance, the heat leakage losses P_{wall} is a function of thermal resistance R_{th}, described by

$$P_{\text{wall}} = \frac{T_{\text{in}} - T_{\text{out}}}{R_{\text{th,eq}}} \tag{4.5}$$

where T_{in} is the inner wall temperature and T_{out} is the outside ambient temperature.

With reference to the heat exchanger optimization presented in the Appendix A, we see that the maximum air temperature allowable inside the chamber, as per Finnfoam specifications is 75℃. Assuming the outside ambient temperature is at 23℃, the calculated maximum wall heat-leakages amount to $P_{\text{wall}} \approx 46$ W.

Copper Heat Leakage

Copper being a very good thermal conductor, the power cables and other copper connecting wires present inside the calorimetric chamber lead to heat leakage. The temperatures at the wire endings are sensed by the Pt-100 elements recorded during the course of the calorimetric test at fixed intervals of time. So, the power lost through or added by the copper conductors in question could simply be denoted as:

$$P_{\text{cu}} = \frac{T_{\text{in}} - T_{\text{amb}}}{R_{\text{cu}}} \tag{4.6}$$

where T_{in} is the temperature at the end inside the test chamber and T_{out} is the temperature at the exposed end. From different tests, it was observed that the conductor end temperatures coincided closely with the inner chamber temperature and the ambient temperatures. So this temperature gradient $T_{\text{in}} - T_{\text{amb}}$ is the same as the one across the walls.

R_{cu} is the equivalent thermal resistance of the copper wires,

$$R_{\text{cu}} = \frac{l}{\kappa A_{\text{cu}}} \tag{4.7}$$

l is the average measured length of the wire
A_{cu} is the copper cross-sectional area
κ is thermal conductivity of copper 401 W/(m·K).

If the temperature of the leads from the power supply (T_{in}) is lower than those of the DUT(T_{out}), then the heat energy is being lost from the calorimeter block by way of the copper thermal conduction. The correction can be applied by adding this power loss ($+P_{\text{cu}}$) to the power balance Eq.(4.5).

Conversely, heat energy is added to the calorimetric chamber if the DUT power leads are cooler than those at the power supply board. The correction then would be to subtract this power gain ($-P_{cu}$) from the power balance equation (4.4). From [10], supposing ΔT_{i} is the average temperature difference during a time interval, the energy gained or lost by N_{cu} copper conductors during any particular time interval (Δint) is,

$$E_{\mathrm{i}} = \frac{\kappa A_{\mathrm{cu}}}{l} N_{\mathrm{cu}} \Delta T_{\mathrm{i}} \Delta int$$

The total energy loss over n time intervals is hence,

$$E = \sum_{i=1}^{n} E_{\mathrm{i}} = \frac{\kappa A_{\mathrm{cu}}}{l} N_{\mathrm{cu}} \Delta int \sum_{i=1}^{n} \Delta T_{\mathrm{i}}$$

But, since the wires used are of a small cross-section, the measurement of the copper wire-end temperatures with the available PT 100 sensors proved to be rather tricky. Also, copper conductors too are simultaneously generating heat losses by way of Joule heating losses or the I^2R. This analysis is important because if the coolant fluid is of a low specific heat capacity (like helium), it will boil away if the temperature coming into the calorimeter through the wire ends is too high.

Hence the energy gained by or lost from the calorimetric chamber through both these mechanisms have to be accounted for. This can be done by analyzing the temperature distribution in the wire during the course of the calorimeter test.

It is assumed that there is no heat flowing radially out through the insulation of the copper wire. The heat flow problem thus reduces to a single dimension, where heat flows only axially, *i.e.* only along the length of the copper wire. Heat power thus will come out at the ends of the wire, either inside the calorimetric chamber or outside at the power supply board. Hence, heat will flow to that end at a lower temperature.

The thermal analysis then reduces to a problem which can be described by the one-dimensional heat equation:

$$T(x) = -\frac{p}{2\kappa} x^2 + Cx + D \tag{4.8}$$

p is the power density in the conductor
x is the position indicator along the length of the wire, at which temperature is calculated
C and D are the parameters that will be obtained from the boundary conditions.

The solution of the 1D heat equation showed, as expected, that the peak temperatures in the conductor increased with current it is carrying. But the simultaneous processes of heating and leakage, do not add or leak much heat from the calorimeter chamber. The details of the solution of the equation and temperature analysis of wire is presented in Appendix B.

Fan Power

Fitted to each radiator, there are six 12V DC fans each of 30 mm diameter with maximum speed of 1200 rpm. The fan energy dissipated in the calorimeter is also measurable electrical energy that should be accounted for in the coolant thermal power increase.

Stray Loss

The losses that are not accounted for by thermal power, wall leakage, fan power and copper loss measurements can be termed as 'stray losses'. These usually arise from various measurement errors and are hard to predict empirically and may not be directly measurable. Even so, it can be defined as being directly proportional to the inner and ambient temperature gradient. With proper calibration and by maintaining a constant ambient temperature throughout the measurement, unwanted measurement errors can be avoided.

$$P_{\text{stray}} = \frac{T_{\text{ch}} - T_{\text{amb}}}{R_{\text{stray}}} \tag{4.9}$$

R_{stray} is the equivalent thermal resistance corresponding to stray power loss P_{stray}.

If the ambient temperature can be stabilised throughout the test process, the stray losses can be minimized to some extent.

Coolant Power

In an ideal situation, the power lost from the DUT is completely absorbed by water. But considering all the various heat leakage losses, the actual power loss from the DUT is measurable only from the power absorbed by the water in the heat exchanger. If the measurement of P_{w} depends on the measurement of different variables $x_1, x_2, ..., x_n$ of the measuring system, then it is a function of those variables, expressed as $P_{\text{w}} = f(x_1, x_2, ..., x_6)$

The specific heat capacity of water coolant and its density is assumed to remain constant during the test. Consequently, the fluid flow rate and the fluid temperature measurement are the independent variables which control the power absorbed by the fluid, as per Eq.(3.2). The error in measurement of the input quantities lead to uncertainty in the final measured value of the power loss, hence the need to estimate the tentative value of the power loss obtained from the measurement. And so, with the knowledge of the accuracy, repeatability and resolution of the measuring meters and sensors of these entities, the overall accuracy of the power measurement can be determined. Hence, the uncertainty in coolant power measurement, as detailed in Appendix C is given by the RPBE technique with the RSS formulation

$$u(P_{\text{w}}) = P_{\text{w}} \sqrt{\left(\frac{u(\Delta T)}{\Delta T}\right)^2 + \left(\frac{u(\dot{V})}{\dot{V}}\right)^2}. \tag{4.10}$$

With reference to Table C.1 which lists the accuracies of the Pt-100 temperature sensors and the flow controller, this can be further written as

$$u(P_{\mathrm{w}}) = P_{\mathrm{w}} \sqrt{\left(\frac{0.0489\ ^{\circ}\mathrm{C}}{\Delta T\ ^{\circ}\mathrm{C}}\right)^2 + \left(\frac{0.866\ \mathrm{ml/min}}{\dot{V}\ \mathrm{ml/min}}\right)^2} \tag{4.11}$$

where $u(P_{\mathrm{w}})$ is the uncertainty in measuring thermal power P_{w} at water flow-rate $\dot{V}$ and water temperature-rise ΔT.

If the estimated value overshoots the maximum allowable measurement error margin which was set at the start, it means that more accurate measurement devices have to be used.

4.6 Data Acquisition Systems

The sensor data from the various Pt-100 temperature sensors deployed in the calorimeter system was acquired with a HP DAQ 349970A Data Acquisition/Switch Unit and read on the PC with the Agilent VEE Pro graphical programming software.

The electrical power supplied to the calorimeter was read at the connection terminals by Fluke Norma 4000 and read with the Agilent VEE Pro software as well.

5 Measurement Results

5.1 Balance Test

The balance test was conducted with a resistor of 15.6 Ω supplied with regulated DC power supply so as to maintain a fixed power dissipation, at different levels ranging from 25 W to 125 W. All the tests were carried out at a constant flow rate of 200 ml/min. All the tests were run until the steady state was achieved. From the measured data of the water temperatures and air, wall temperatures the thermal power and leakage calculations were carried out.

The steady-state analysis of the measurement system was done as per the standard IEC 34-2A (1972). It states that, stable conditions are achieved when "measurements of rise in temperature and volume flow rate of cooling medium indicate that losses are constant to within ±1% over a period of two hours or when the temperature rise of the cooling medium does not vary by more than ±1% in one hour, the volume flow rate being constant."

Both these steady-state requirements were considered simultaneously to check the stability of the measurements. The setting times ranged from 4-12 hours. The time taken for the system to stabilise increased as the measured electrical power decreased. Once the steady state was reached, the sensor data collected from the various balance test-runs were used to calculate the thermal power gained by the coolant respective to the electrical power. The electrical power measurement included the fan power also, which amounted to $P_{\text{fan}} \approx 8$ W.

The calorimeter calibration curve was then constructed by fitting a curve to the measured values. The fitting was accomplished with polynomial fitting which works in a least-square sense. This curve, which denotes the relation between the total power dissipated inside the calorimeter and the coolant thermal power; eliminates the need to run the balance test every time the DUT has to be tested.

The linear relationship between the electrical power and the thermal power obtained is

$$P_{\text{w}} = 0.88 P_{\text{loss}} - 1.27 \text{ W}. \tag{5.1}$$

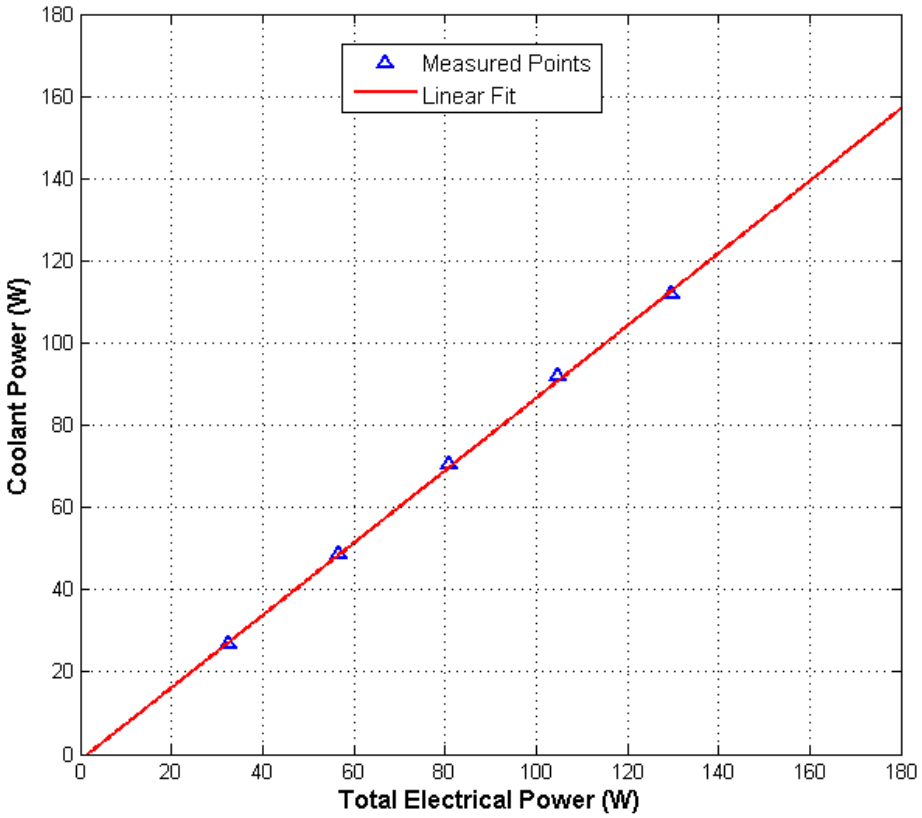

Figure 5.1: Calibration curve relating the total electrical power and coolant thermal power.

Only 88% of the power dissipated by the DUT is being absorbed by the coolant. The measured thermal powers were falling short of the electrical power by a couple of watts. The wall leakages were computed in every case, and as expected, it was observed that the leakages increased proportionally with the electrical power being measured. For every extra 25 W of electrical power measured, the wall leakages increased by approximately 3 W. By calculating the wall leakages and finding out the effective net temperature rise of water, wall leakage losses were compensated. A new calibration curve was plotted.

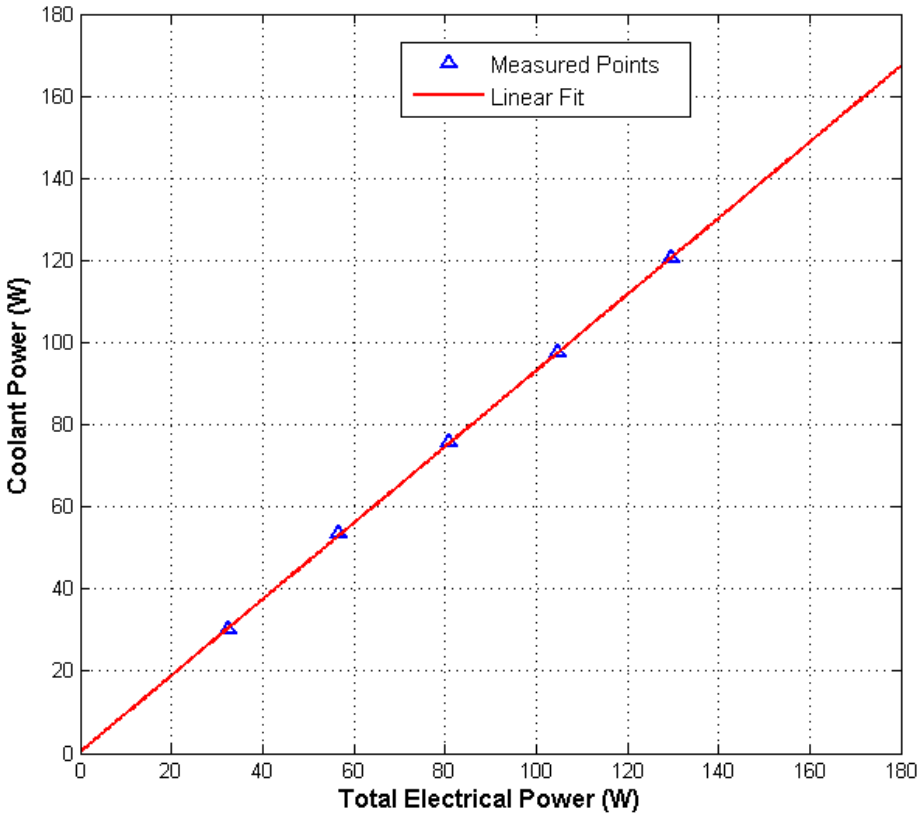

Figure 5.2: Calibration curve for compensated thermal power.

The equation (5.1) then reforms into

$$P_{\mathrm{w}} = 0.946 P_{\mathrm{loss}} + 1.077 \text{ W}. \tag{5.2}$$

The correlation coefficient is the measure of how good or bad the curve fit is. The computed correlation coefficient in this case was 1, indicating a good fit. The error in the curve fit is shown in Figure 5.3.

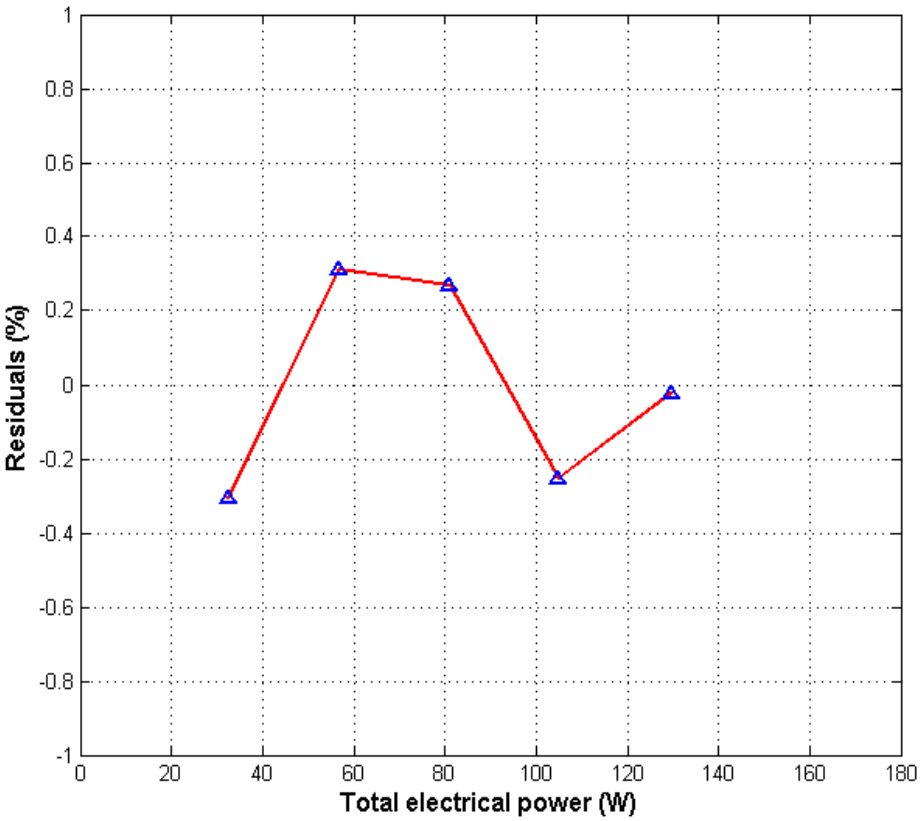

Figure 5.3: Error in the curve fitting.

The calibration curve presented here was at a constant flow rate of 200 ml/min. The variation of water temperature rise with its flow-rate at different water thermal powers follows the relationship described in equation (3.2) and is illustrated in Figure 5.4. For a different water flow rate, the balance tests have to be carried out again at various power levels to calibrate the system.

Since the calibration curve defines and predicts the temperature rise of the coolant at a particular flow rate for different power dissipation, the calorimeter test on the device can be conducted directly. The measured results from the DUT test can then be correlated with the calibration curve to determine the electrical power lost by the DUT. The plot on Figure 5.4. can be consulted for the choice of the appropriate water flow-rate.

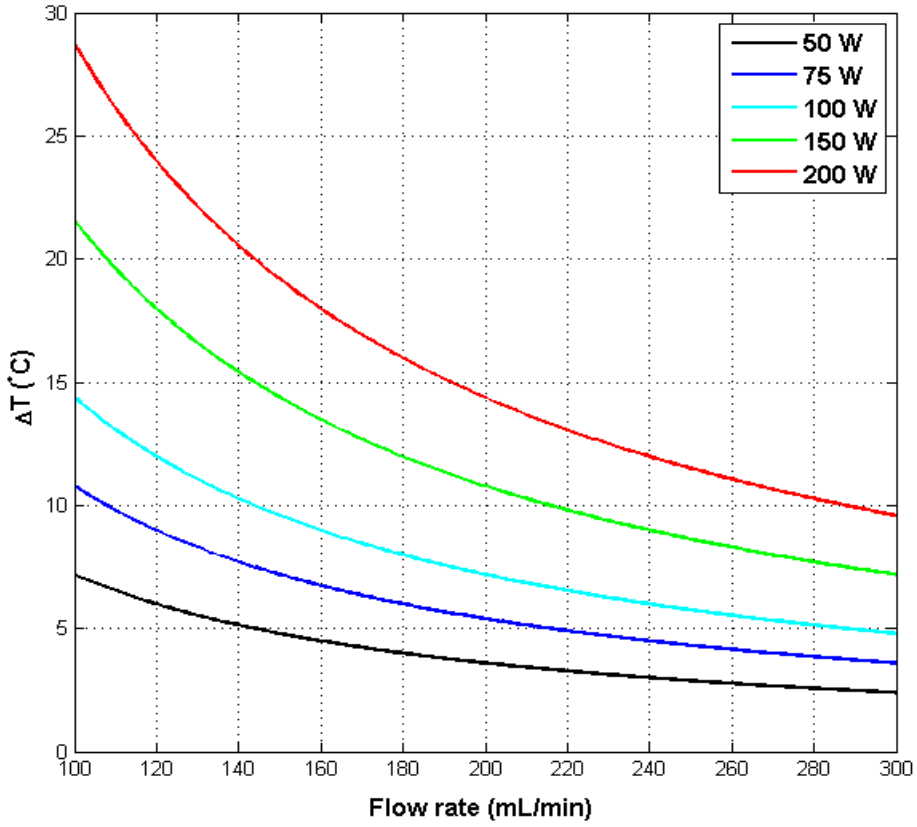

Figure 5.4: Variation of temperature rise with coolant flow rate.

5.2 Actual Test

The actual test was carried out with ABB frequency converter ACS 350-01E-04A7-2. The converter was loaded with a 3-phase resistor and supplied with 230V, at 50 Hz.

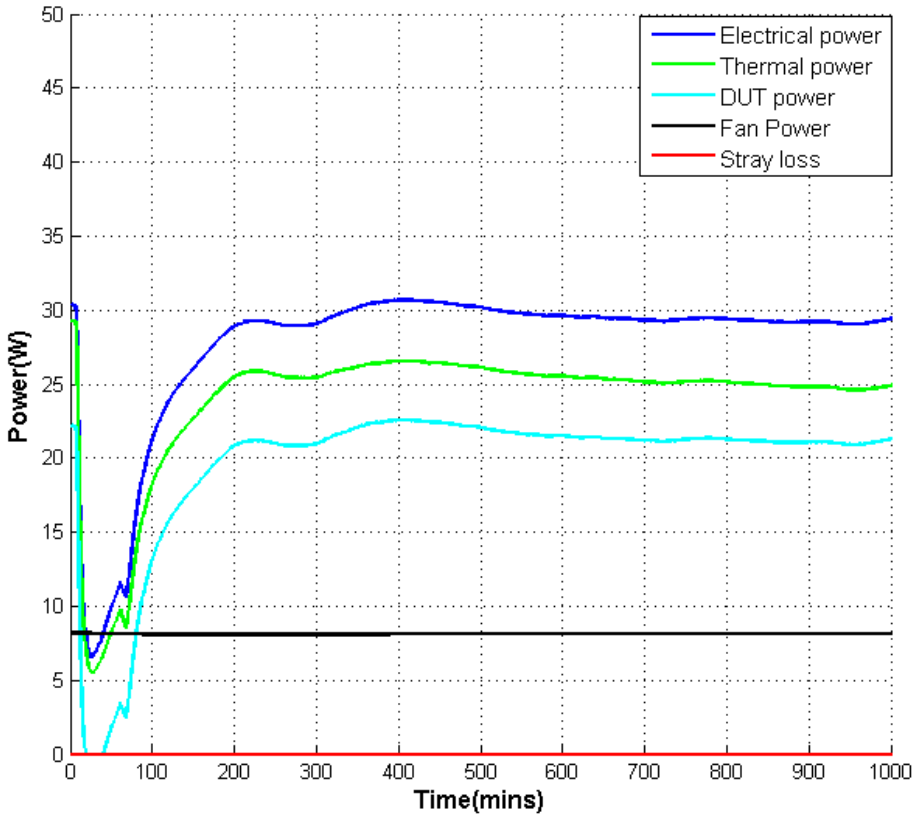

Figure 5.5: The powers measured from the calorimeter test of the frequency converter.

The thermal power curve indicates the power absorbed by water (P_{w}), calculated from the measured water temperature rise and the volume flow rate. The wall leakage losses P_{wall} were calculated from the wall temperatures measured. Summing the thermal power and the wall heat leakage, the total electrical power that was dissipated in the calorimeter is obtained, which is $P_{\mathrm{loss}} + P_{\mathrm{fan}}$. The actual power lost by the DUT P_{loss} is then found by deducting the fan power P_{fan}, which was measured to be around 8 W. Copper conductor heat leakages P_{cu} calculated were very less and hence neglected.

So, assuming wall-leakage compensation (when the walls did not leak heat), the average power lost by the frequency converter $P_{\mathrm{loss}} \approx 21.35$ W. Separate electrical measurements of the DUT power showed that the frequency converter was consuming 0.75 kW of electrical power. The output power was around 0.727 kW which

indicated power losses of about 23 W. This implies that the DUT has an efficiency of around 97%.

6 Discussion

The attempt at measuring the power loss of the frequency converter with the calorimeter that was built was fairly successful. The water input temperature control that was implemented was efficient and ensured a fairly constant temperature of the incoming water stream over the course of one measurement. The performance of the flow controller, was also verified to be satisfactory.

Nevertheless, the intention to prevent wall leakage with the extra insulation thickness along the walls, has not seen fruition. Although increasing the wall thickness did increase the thermal resistance along the heat paths through the walls, the effective thermal resistance of the calorimeter as a whole was low. The thermal conductivity of the insulation slabs too was higher than expected. Hence the wall leakage losses were considerable, and were the most prominent cause of error in the thermal power measurement. Higher the electrical power being measured, higher were the wall leakages. However, they could be reasonably assessed with the accurate measurement of the wall temperatures by the Pt-100 sensors. Furthermore, the accuracy of the temperature measurements can be improved by achieving a higher temperature rise.

The losses observed in the measurements, not accounted for by the wall leakages maybe owing to the leakages happening due to imperfections in the construction of the box. There could be heat leaking out through the gaps between the 2 shells of the calorimeter. These leakages are difficult to isolate and cannot be measured easily. They can hence be termed as the stray losses in the system. Copper conductor losses, were found not to contribute much to the thermal power measurement errors. At higher powers, dimensioning of the conductors can be optimised to diminish copper heat leakages.

The settling times observed were fairly large, especially while measuring lower powers. A main reason behind this is the changing ambient temperature of the hall where the calorimeter was located. Fluctuating surrounding temperatures during the course of the measurement affect the leakage patterns in the system and prevent it from stabilising, and also induce measurement errors. The high wall thickness was also not helping the system to achieve stable state quickly.

6.1 Conclusion and Future Work

With the current flow controller system, the maximum power loss that can be measured by the calorimeter is 520 W. This calorimetric watt meter system can be used to test not only small frequency converters, but also devices which have minimum losses of at least 25 W, provided the DUT is small enough to fit in the calorimeter chamber.

A better design and precise construction of the insulation box that makes up the calorimeter will, by all means prevent any sort of unwanted leakages from happening. As far as the wall leakages are concerned, increasing the wall thickness alone may not always eradicate the losses since a really thick insulation comes at the cost of high measurement settling times. Also, ensuring a near-constant ambient temperature,

albeit a difficult task, will prevent rogue errors in measurement from occurring.

Thanks to the highly accurate temperature sensors and flow control system, the system can measure power losses n the range of 25 W - 520 W with a fairly good accuracy. For 25 W of power measured, the extended uncertainty in measurement is approximately 0.5% at 200 ml/min flow rate. Beyond 75 W of losses measured, the extended uncertainty is at least 2%. Although not as effective as the double jacketed calorimeter in countering the wall leakages, this calorimeter, even without the double jacket and air-gap temperature control of the DJC, can be made more accurate. This can be done through a more thorough initial design process, to optimise the dimensioning and the choice of the wall insulation material and its thickness.

Keeping in mind the measurement capacity of this closed, water cooled calorimeter; it is probably a bit too large for measuring precisely the losses of devices with minimum efficiency of 90%, belonging to power class $<$ 1kW. Also since the calorimeter is meant for small devices, with a smaller and better dimensioning of the calorimeter box, it is very viable to target and achieve the intended measurement accuracy. For this to succeed, the design process should only proceed once the dimensions of the heat exchanger, balance resistor and DUT are known in advance. Choosing an appropriately dimensioned heat exchanger for transferring the power intended is also then an important design challenge. This closed water-cooled calorimeter, by way of its stretched measurement range is now more versatile. Also, the water temperature rise control schema can be implemented, and tested for its effectiveness over the input water temperature control scheme.

There is no refrigeration system installed in this calorimeter and so it is unsuited for processes that take place below a certain ambient temperature. Additionally, a water cooling system will help save on water, and avoid unnecessary wastage by cooling the warm water from the calorimeter and subsequently circulating the cooled water back into the system.

7 References

[1] Cao, W., Asher, G. M., Huang, H., Zhang, H., French, I., Zhang, J. and Short, M. "Calorimeters and Techniques Used for Power Loss Measurements in Electrical Machines", *IEEE Instrumentation & Measurement Magazine*, vol. 13, no. 6, pp. 26-33, Dec. 2010.

[2] Jain, A. M., Ayyanar, R. Section 22 Power Electronics, [Cited 29 Jan. 2013], Available at: http://books.mcgraw-hill.com/engineering/PDFs/Beaty_Sec22.pdf

[3] Erickson, R. W. "Fundamentals of Power Electronics, Accompanying material for Instructors", *Fundamentals of Power Electronics Instructor's Slides*, [Cited 29 Jan. 2013], Available at: http://cs5824.userapi.com/u11728334/docs/5791ef177f3b/Robert_W_Erickson_FUNDAMENTALS_OF_POWER_ELECTRO.pdf

[4] Zhang, W., Liu, Y., Li, Z. and Zhang, X. "The Dynamic Power Loss Analysis in Buck Converter", *Proc. IEEE 6th International Conf. Power Electronics and Motion Control Conference*, pp. 362-367, May 2009.

[5] Turner, D. R., Binns, K. J., Shamsadeen, B. N. and Warne, D. F. "Accurate measurement of induction motor losses using balance calorimeter", *Proc. IEEE*, vol. 138, no. 5, pp. 680-685, Sep. 1991.

[6] Lindström, J. "Calorimetric methods for loss measurements of small cage induction motors", *Master's Thesis*, Espoo, Helsinki University of Technology, Faculty of Electrical Engineering, Laboratory of Electromechanics, Otaniemi, 1994.

[7] Jalilian, A., Gosbell, V. J., Perea, B. S. P. and Cooper, P. "Double chamber calorimeter (DCC): a new approach to measure induction motor harmonic losses", *IEEE Transactions on Energy Conversion*, vol. 14, no. 3, pp. 680-685, Sep. 1999.

[8] Singh, D. "Calorimetric Measurement of the Stator Core Losses Caused byManufacturing", *Master's Thesis*, Aalto University, School of Electrical Engineering, Faculty of Electromechanics, Otaniemi, 2011.

[9] Rasilo, P., Ekström, J., Haavisto, A., Belahcen, A. and Arkkio, A. "Calorimetric System for measurement of synchronous machine losses", *IET Electric Power Applications*, vol. 6, no. 5, pp. 286-294, May 2012.

[10] Bowman, J. K., Cascio, R. F., Sayani, M. P. and Wilson, T. G. "A Calorimetric Method for Measurement of Total Loss in a Power Transformer", *Proc. 22nd Annual IEEE Power Electronics Specialists Conference*, pp. 633-640, June 1991.

[11] Bradley, K. J., Cao, W., Arellano-Padilla, J. "Evalutaion of Stray Loss in Induction Motors With a Comparison of Input-Output and Calorimetric Methods", *IEEE Transactions on Energy Conversion*, vol. 21, no. 3, Sep. 2006.

[12] Christen, D., Badstuebner, U., Biela, J. and Kolar, J. W. "Calorimetric Power Loss Measurement for Highly Efficient Converters", *Proc. International Power Electronic Conference*, pp. 1438-1445, June 2010.

[13] Weier, S., Shafi, M. A. and McMahon, R. "Precision Calorimetry for the Accurate Measurement of Losses in Power Electronic Devices", *Proc. IEEE Industry Applications Society Annual Meeting*, pp 1-7, Oct. 2008.

[14] Malliband, P. D., van der Duijn Schouten, N. P. and McMahon, R. A. "Precision Calorimetry for the Accurate Measurement of Inverter Losses", *Proc. 5th Int. Conf. Power Electronic Drives and Systems*, 2003, vol. 1, pp. 321-326, Nov. 17-20.

[15] Blaabjerg, F., Pedersen, J. K. and Ritchie, E. "Calorimetric measuring systems for characterizing high frequency power losses in power electronic components and systems",*Proc. IEEE Industry Applications Conference*, vol. 2, pp. 1369-1376, Oct. 2002.

[16] Kamei, R., Tae-Woong, K. and Kawamura, A. "Accurate Calorimetric Power Loss Measurement for Efficient Power Converters", *Proc. IECON 2011-37th Annual Conference on IEEE Industrial Electronics Society*, pp. 1173-1178, Nov. 2011.

[17] Hansen, P., Blaabjerg, F., Mansen, K. D., Pedersen, J. K., Ritchie, E. "An Accurate Method for Power Loss Measurements in Energy Optimized Apparatus and Systems.", [Cited 29 Jan. 2013], Available at: http://vbn.aau.dk/files/62037985/an_accurate_method_for_power_loss_measurements.pdf

[18] Xiao, C., Chen, G., Odendaal, W. G. H. "Overview of Power Loss Measurement Techniques in Power Electronic Systems", *IEEE Transactions on Industry Applications*, pp. 657-664, May-June 2007.

[19] Ammous, K., Allard, B., Garrab, H. and Ammous, A. "Losses Evaluation in Converters using the Calorimetric Technique", *Journal of Thermal Analysis and Calorimetry*, vol. 90, no. 1, pp. 307-314, Oct. 2007.

[20] Carastro, F., Clare, J. C., Bland, M. J., Wheeler, P. W. "Calorimetric loss measurements and optimization of high power resonant converters for pulsed applications", *Proc. 14th European Conference on Power Electronics and Applications (EPE 2009)*, Sept. 2009.

[21] Dimitrakakis, G. S., Tatakis, E. C., Nanakos, A. Ch. "A simple calorimetric setup for the accurate measurement of losses in power electronic converters", *Proc. 14th European Conference on Power Electronics and Applications (EPE 2011)*, Sept. 2011.

[22] Forest, F., Huelstein, J-J., Faucher, S., Elghazouani, M., Ladoux, P., Meynard, T. A. "Use of Opposition Method in the Test of High-Power Electronic Converters", *IEEE Transactions on Industrial Electronics*, pp. 530-541, April 2006.

[23] Cao, W., Bradley, K. J., French, I., Zhang, J. and Zhang, H. 'A Review of Calorimetric Application for Accurate Power Loss Measurement", *Proc. of the 41st International Universities Power Engineering Conference UPEC '06.*, pp. 550-554, Sep. 2006.

[24] Cao, W. 'Comparison of IEEE 112 and New IEC Standard 60034-2-1", *IEEE Transaction on Energy Conversion.*, vol. 24, no. 3, pp 802-808, Sep. 2009.

[25] Sridhar, S., Wolf, R. M., Odendaal, W. G. "An Accurate Experimental Apparatus for Measuring Losses in Magnetic Components", *Proc. IEEE 34th IAS Annual Meeting*, vol. 3, pp. 2129-2133, 1999.

[26] Chen, G., Xiao, C., Odendaal, W. G. "An Apparatus for Loss Measurement of Integrated Power Electronics Modules: Design and Analysis", *Proc. 37th IAS Annual Meeting Industrial Applications Conf.*, vol. 1, pp. 222-226, Oct.2002.

[27] Kuebrich, D., Goettle, J., Duerbaum, T. "Power Loss Measurement based on Transient Temperature Rise", *Proc. 27th IAS Annual Applied Power Electronics Conference and Exposition.*, pp. 1797-1801, Feb.2012.

[28] EA-4/02, W. 'Expression of the Uncertainty of Measurement in Calibration", *European co-operation for Accreditation EA-4/02.*, Dec. 1999.

[29] Oetiker, T., Partl, H., Hyna, I. and Schlegl, E. "The Not So Short Introduction to LaTeX 2ε", Version 5.01, April 06, 2011. [Cited 29 Jan. 2013], Available at: http://tobi.oetiker.ch/lshort/lshort.pdf

A Heat Exchanger Optimisation

For the heat exchange mechanism to be ideal, the power absorbed by air in the test chamber from the DUT should equal the heat absorbed by the water circulated in the heat exchanger. That is,

$$\begin{aligned} P_{\mathrm{a}} &= P_{\mathrm{w}} \\ (\rho \dot{V} c_p \Delta T)_{\mathrm{a}} &= (\rho \dot{V} c_p \Delta T)_{\mathrm{w}} \\ (C \Delta T)_{\mathrm{a}} &= (C \Delta T)_{\mathrm{w}} \end{aligned}$$

The measure of performance of a heat exchanger is its 'Effectiveness' ϵ, which is the ratio between actual heat transfer and the maximum possible heat transfer according to the second law of thermodynamics.

$$\epsilon = \frac{P}{P_{\max}} = \frac{P_{\mathrm{a}} = P_{\mathrm{w}}}{\min(C_{\mathrm{a}}, C_{\mathrm{w}}) \cdot (T_{\mathrm{Ahot}} - T_{\mathrm{Acold}})} \tag{A.1}$$

where,

P_{a} is the power transferred from air.
P_{w} is the power absorbed by water.
C is the Heat capacity rate defined as, $C = \rho \dot{V} c_p$.
T_{Ahot} is the hot air temperature entering the heat exchanger.
T_{Acold} is the cold air temperature exiting the heat exchanger.
T_{Wcold} is the cold water temperature entering the heat exchanger.
T_{Whot} is the hot water temperature exiting the heat exchanger.

The effectiveness expected from the heat exchanger in question is less than the ideal which is 1. The inlet and outlet air and water temperatures are to be optimized considering various aspects of heat exchange mechanism between the hot air and cold water streams.

As per the data provided by the manufacturers, at full speed of the DC fans which ensure air flow, the thermal resistance of the heat exchanger is about 0.04 K/W. The maximum temperature that the Finnfoam sheets can stand is 75℃. So restricting the maximum allowable temperature for the air inside the calorimeter be 70℃. If the inlet water stream temperature is maintained at, $T_{\mathrm{Wcold}} = 15$℃, then the maximum power that can be transferred with 2 heat exchangers is

$$P_{\max} = \frac{70\text{℃} - 15\text{℃}}{R_{\mathrm{th,he}}} = 688 \text{ W}.$$

Accordingly, the maximum water temperature rise at the maximum flow rate of 300 ml/min will be approximately 33℃. For an inlet water temperature of 15℃, this would mean that the out-coming water is at 48℃.

The upper limit to the water temperatures should be fixed according to the pipes that carry it. So, by fixing the upper limit of water temperature to 40℃, the maximum power that can be transferred at the maximum flow-rate of 300 ml/min is approximately 522 W (assuming $\epsilon = 1$). Air volume flow rate generated by the

fans is 0.015 m^3/s. If the ambient $T_{Acold} = 23℃$, then for $P_a = 522$ W, $T_{Ahot} = 52℃$. Air has lower thermal capacity than water $C_a < C_w$.

The air and water hot stream's maximum temperatures at the maximum flow rate 300 ml/min are thus:

$T_{Ahot} = 52℃$ and $T_{Acold} = 23℃$.
$T_{Wcold} = 40℃$ and $T_{Whot} = 15℃$.

B Copper Heat Loss

The free electrons in metals transport not only electricity, but also heat. Metals like copper which are very good electrical conductors are hence good thermal conductors also.

The length and type of the copper wires leading out from the calorimeter were noted. With a standard look-up table, the electrical resistance and cross-sectional area corresponding to the American Wire Gauge (AWG) classes of the wire can then be found. Net electrical resistance of the copper wire can be measured with a multimeter as well. The measured data for calculating copper leakages is presented here.

Table B.1: Measured copper wire data.

Connections	**Cu cross-section** ($\times 10^{-6}$ m^2)	**Length** (m)	**Electrical resistance per meter** (Ω/m)	**No. of wires**
DUT	2.08	1.85	8.286	5
Resistor	1.31	1.925	13.17	2
DC fans	0.326	2.42	52.96	4

The one-dimensional heat equation describes the axial heat flow in copper conductors

$$T(x) = -\frac{p}{2\kappa}x^2 + Cx + D, \tag{B.1}$$

where $\kappa = 401$ W/(m·K) is the thermal conductivity of copper.

If L is the total length of the copper wire and x indicates the position along the wire, the boundary condition $x = 0$ yields D= 18.48℃. This is the measured temperature of the wire end exposed to ambient. $T(L)$ is the temperature at the other which is inside the calorimeter, which is obtained from measurements. p is the power density of the wire; given by the ratio of the I^2R losses in the wire to its area of cross-section.

Solving this differential equation to obtain the temperatures at successive points along the length of the wire, a plot similar to the Figure B.1 can be obtained. The slope of the curve gives the power leaked or added

$$P_{\text{cu}} = -\kappa A_{\text{cu}} N_{\text{cu}} \cdot \frac{\Delta T}{\Delta x}.$$

If the maxima lies at the midpoint of the curves, it can be concluded that heat is flowing in both directions towards both ends. If the temperature at one end of the wire is greater than at the other, the maxima of the parabolic distribution shifts towards that end, and there will be a net heat leakage happening.

The figure below shows the parabolic temperature distribution of copper wires while the balance test at 25 W of electrical power was carried out. It was observed

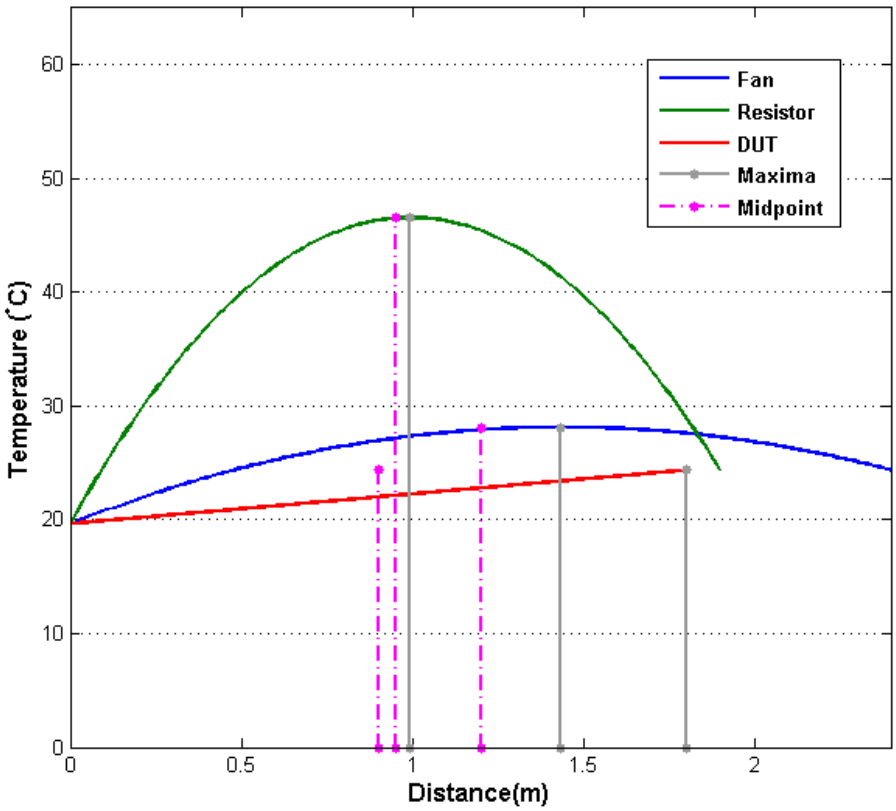

Figure B.1: Solution of 1-D heat equation in copper conductors.

that the resistor wires, which carries more current reaches the highest peak temperature almost at the midpoint of the wire. This implies that the heat flows from this high point to both ends of the wire and thus in effect, adding as well as leaking heat from the calorimeter chamber. But the power leaked is the same as the power added and so the effect of the resistor conductors on heat leakages in negated. The DUT wires which are not carrying any current during the balance test and the fans conductors do leak heat from the chamber. The heat they leak is negligible though.

The temperature analysis of the conductors during tests at different power levels was done and similar results were obtained in all cases. It was found that the heat leaks are not very substantial, amounting from 0.01 W to maximum 0.15 W. Higher copper leakage losses can be mitigated by altering the area of cross-section w.r.t. the length of the wire used. It is then, a trade-off between the heat leakages and Joule heating losses.

C Uncertainty in Power Measurement

The overall measurement error in any scientific measurement can be categorised into three components: instrumental errors, methodological errors and human errors. These three in conjunction determine the accuracy of the measurement undertaken. The factors contributing to instrumental as well as methodological errors are instrument accuracies, methodology of testing procedures; as prescribed by standards or specifications. Human errors are due to mistakes made in carrying out the test, taking measurements and processing results by the persons in charge. Human errors are difficult to avoid also to quantify, unless all the personnel had the exact same measurement instrument, test rig and measurement process throughout.

The human error component can be neglected and the remaining error components can be attempted to be estimated with any of the following procedures. There are existing, two methods for evaluating measurement uncertainty [24]:

• **Worst case estimation** (WCE): This method of uncertainty computation took into account all the maximum possible instrumental error, thus overestimating the overall measurement inaccuracy.

• **Realistic perturbation-based estimation** (RPBE): This method is am improvement to the WCE and tackles the former's shortcoming by considering the different weight each individual factors/measurements carry in the measurement process, w.r.t their instrumental accuracy. Each individual uncertainty contribution is then combined by quadrature summation or the Root Sum of the Squares Method (RSS). This is the method adopted in this work and has been explained further on.

RPBE

RPBE makes use of the root sum squared (RSS) method to calculate the aggregate accuracy of a measurement when the accuracies of all the measuring devices are known. And since accuracy and uncertainty are used interchangeably, the uncertainty results yield the accuracy of the calorimeter as well.

The final quantity being measured in the calorimetric process is the Power loss of the DUT. Power loss measurement however, depends on the water coolant's temperature rise and its volume flow rate measurements. The specific heat capacity and density of water is assumed not to change during the measurement process. Thus the measurement uncertainty in the water temperature and the flow rate directly affect the uncertainty in the Power loss measurement as well.

If Y is the output measurand which depends on multiple input variables $x_1, x_2, ..., x_n$, then the functional relationship between the input parameters and the output Y can be described as

$$Y = f(x_1, x_2, ..., x_n).$$

As per the rules defining the propagation of errors, the general equation for standard uncertainty of the output measurand Y, expressed as $u(Y)$ depends on sum of squares of the weighted measurement uncertainty of each of the input variables. $u(x_1)$, $u(x_2)$ are the standard uncertainties (standard deviations) in measurement due to random instrumental errors of the input variables $x_1, x_2, .., x_n$.

Unlike in type A evaluation of standard uncertainty using statistics, our case is a Type B scenario wherein, the uncertainty estimates are obtained from the manufacturer's specifications of the measuring instruments used. Since we lack statistical data, it is difficult to predict if the measurement data will follow any of the distributions- rectangular, triangular, normal or any other kind. But the information that is available though, is the error range $\pm\alpha$ specified by the manufacturer. Since there is good probability of the actual measurement value to lie anywhere between this range, it will be a rectangular (uniform) distribution. For a rectangular distribution, the standard uncertainty is obtained as $\frac{\alpha}{\sqrt{3}}$.

The general equation for the uncertainty in measurement of measurand Y is

$$u(Y) = \sqrt{{c_1}^2 u(x_1)^2 + {c_2}^2 u(x_2)^2 + ... + {c_\mathrm{n}}^2 u(x_\mathrm{n})^2} \tag{C.1}$$

where, $c_1, c_2..c_\mathrm{n}$ are called the sensitivity coefficients. A small disturbance δx_i in the input variable x_i results in a small disturbance δY_i in the output variable Y. Assuming $\delta x_\mathrm{i} \approx u(x_\mathrm{i})$, each independent parameter's contribution to uncertainty is the square of the associated uncertainty expressed as standard deviation multiplied by the relevant sensitivity coefficient.

The sensitivity coefficient dictates to what extent each measurement uncertainty affects the overall uncertainty and is defined as $c_i = \partial Y/\partial x_i$ at x_i.

With reference to equation (3.2), the power gained by the water coolant can be expressed as:

$$P_\mathrm{w} = k\Delta T\dot{V} = k(T_\mathrm{o} - T_\mathrm{i})\dot{V} = f(T_\mathrm{o}, T_\mathrm{i}, \dot{V})$$

where k is a constant term which stands for the product of c_p and ρ. f represents the non-linear relationship between the input parameters $T_\mathrm{o}, T_\mathrm{i}, \dot{V}$ and the output, P_w. Now,

$$\Delta T = T_\mathrm{o} - T_\mathrm{i}$$
$$\therefore u(\Delta T) = \sqrt{u(T_\mathrm{o})^2 + u(T_\mathrm{i})^2}.$$

Hence, the combined uncertainty is;

$$u(P_\mathrm{w}) = P_\mathrm{w}\sqrt{\left(\frac{u(\Delta T)}{\Delta T}\right)^2 + \left(\frac{u(\dot{V})}{\dot{V}}\right)^2}.$$

If the variables are in some way dependent(correlated to some degree), then their covariance also has to be considered as a contribution to the uncertainty. But the water volume flow rate and temperature rise measurements happen independently with different instrument which suffer from different instrumental as well as random errors, and so the covariance term is zero.

Table C.1: Uncertainty of variables.

Quantity (x_i)	**Estimate**	**Error Range** $\pm\alpha$	**Standard Uncertainty** $u(x_i)$
Inlet Water Temperature (T_i)	15 ℃	±0.06 ℃	0.0346 ℃
Outlet Water Temperature (T_o)	20 ℃	±0.06 ℃	0.0346 ℃
Water Flow Rate ($\dot{V}$)	216 ml/min	1.5 ml/min	0.8660 ml/min
Inside Air Temperature (T_i)	15 ℃	±0.03 ℃	0.0173 ℃
Outside Air Temperature (T_i)	15 ℃	±0.03 ℃	0.0173 ℃

Table C.2: Uncertainty of different functions.

Function Y	**Combined Uncertainty** $u(Y)$
$Y = x_1 \pm x_2$	$u(Y) = \sqrt{u(x_1)^2 + u(x_2)^2}$
$Y = kx_1x_2$	$u(Y) = Y\sqrt{(u(x_1)/x_1)^2 + (u(x_2)/x_2)^2}$

$\therefore$ The combined standard uncertainty due to water temperature difference ΔT and flow rate measurements in power absorbed by water (P_w) is calculated as

$$u(\Delta T) = \sqrt{(0.0346\ ℃)^2 + (0.0346\ ℃)^2} = 0.0489\ ℃$$

$$\therefore \frac{u(P_\mathrm{w})}{75\ \mathrm{W}} = \sqrt{\left(\frac{0.0489\ ℃}{5\ ℃}\right)^2 + \left(\frac{0.8660\ \mathrm{ml/min}}{216\ \mathrm{ml/min}}\right)^2}$$

$$\therefore u(P_\mathrm{w}) = 0.7939\ \mathrm{W} \approx 1.05\%.$$

Measurement uncertainty is about ±0.8 W when measuring power loss of 75 W.

Expanded Uncertainty: The combined uncertainty which was calculated was for an unspecified confidence level. To present the result with a certain level of confidence say, 95%, the uncertainty result has to be re-scaled by multiplying with a 'Coverage Factor'. The product of this computation is referred to as 'Expanded Uncertainty', which refers to a larger interval which will include a greater portion of the measured values of the measurand P_w. Usually, the combined uncertainty is considered to follow the normal distribution which is, a fair assumption in most cases. So for a confidence level of 95 %, a coverage factor of $K = 2$ is chosen.

$\therefore$ The expanded uncertainty of calorimetric power loss measurement from the power absorbed by coolant $P_\mathrm{w} = 1.58\ \mathrm{W} \approx 2.12\%$ at 75 W.